IEEE Access
practical innovations : open solutions

Received April 16, 2013, accepted April 23, 2013, date of publication June 10, 2013, date of current version June 25, 2013.

Digital Object Identifier 10.1109/ACCESS.2013.2267611

Statistical and Domain Analytics Applied to PV Module Lifetime and Degradation Science

LAURA S. BRUCKMAN[1], NICHOLAS R. WHEELER[2], JUNHENG MA[3], ETHAN WANG[4], CARL K. WANG[4], IVAN CHOU[5], JIAYANG SUN[3], AND ROGER H. FRENCH[6] (Member, IEEE)

[1]Department of Material Science and Engineering, Case Western Reserve University, Cleveland, OH 44106, USA
[2]Department of Macromolecular Science and Engineering, Case Western Reserve University, Cleveland, OH 44106, USA
[3]Department of Epidemiology and Biostatistics, Case Western Reserve University, Cleveland, OH 44106, USA
[4]Underwriters Laboratories, Northbrook, IL 60062, USA
[5]Neo Solar Power Corporation, Hsinchu 30078, Taiwan
[6]Departments of Material Science and Engineering, Macromolecular Science and Engineering and Physics, Case Western Reserve University, Cleveland, OH 44106, USA

Corresponding author: R. H. French (roger.french@case.edu)

ABSTRACT A better understanding of the degradation modes and rates for photovoltaic (PV) modules is necessary to optimize and extend the lifetime of these modules. Lifetime and degradation science (L&DS) is used to understand degradation modes, mechanisms and rates of materials, components and systems to predict lifetime of PV modules. A PV module lifetime and degradation science (PVM L&DS) model is an essential component to predict lifetime and mitigate degradation of PV modules using reproducible open data science. Previously published accelerated testing data from Underwriter Laboratories on PV modules with fluorinated polyester backsheets, which included eight modules that were exposed up to 4000 hrs of damp heat (85% relative humidity at 85 °C) and eight exposed up to 4000 hrs of ultraviolet light (80 W/m^2 of 280–400 nm wavelengths at 60 °C) (UV preconditioning) were used to determine statistically significant relationships between the applied stresses and measured responses. There were 15 different variables tracking aspects of system performance, degradation mechanisms, component metrics and time. Modules were analyzed for three system performance metrics (fill factor, peak power, and wet insulation). The results were statistically analyzed to identify variable transformations, statistically significant relationships (SSRs) and to develop the PVM L&DS model informed by a generalization of structural equation modeling techniques. The SSRs and significant model coefficients, combined with domain analytics, incorporating materials science, chemistry, and physics expertise, produced a pathway diagram ranking the variables' impact on the system performance, which were iteratively examined using sound statistical analysis and diagnostics. The SSRs determined from the damp heat exposure for the system response of Pmax corresponded to the degradation pathway of polyester terephthalate (PET) and ethylene vinyl acetate (EVA) hydrolysis. A linear change point for the damp heat exposure with the system response of Pmax was determined to be 1890 hrs. The UV preconditioning exposure did not induce sufficient degradation shown by the quality of the R^2 values for many of the best fitting models. This exemplifies the development of a methodology to determine rank ordered lifetime and degradation pathways present in modules and their effects on module performance over lifetime.

INDEX TERMS Photovoltaics, statistical analytics, lifetime and degradation science, structural equation modeling.

I. INTRODUCTION

A recent U.S. Department of Energy workshop on Science for Energy Technologies [1] identified photovoltaics (PV) lifetime and degradation science (L&DS) [2]–[4] as a critical scientific challenge for robust adoption of PV. The PVQA Task Force was developed as an international task force to work towards defining what is needed for lifetime qualification standards and tests [5]. Developing and defining useful lifetime qualification standards and tests is complicated since even single degradation modes, mechanisms and rates are not clearly understood and two factor effects are even more complex. Therefore, a methodical domain and statistical

approach is necessary to cross-correlate stressors, degrees of stress and degradation modes, mechanisms and rates for materials, components and systems. This cross-correlation can help provide a better understanding of degradation and lifetime performance in order to guarantee the minimal 25-year lifetime performance of PV modules [6].

A. RELIABILITY AND PROGNOSTIC APPROACHES

The conventional method to determine the reliability of a system or component was to collect failure data and use a single, dominant and constant failure rate to account for product quality and environmental conditions. However, this approach is inaccurate at determining field failure rates and does not produce reliable lifetime predictions [7]–[12]. In contrast, the physics of failure approach, based on failure modes and mechanisms as a function of the stress conditions, provides useful reliability information. The prognostics and health management approach assesses the reliability under application conditions and over lifetime. The combination of the physics of failure and prognostic approaches allows for continuous improvement of lifetime prediction [9], [10], [12]–[21].

B. LIFETIME AND DEGRADATION SCIENCE APPROACH

A practical lifetime approach must consider system response, levels of response and degradation rates under stress conditions that include variable conditions differentiated by region and single, multi-factor, constant and cyclic conditions. This lifetime approach must also cross-correlate real-world and accelerated exposures [22]–[24]. We propose and develop a PV module lifetime and degradation science model (PVM L&DS) using an unbiased analytical approach (combined with both sound statistical analysis and proven domain knowledge and refined iteratively with the latest evidence) and encompassing a comprehensive set of degradation pathways aimed at determining the lifetime of current and next generation technologies.

A stress and response (R(S)) framework links stresses to observed responses, subsequent degradation and damage accumulation over the lifetime of PV materials, components and systems. Stressors can be characterized in terms of instantaneous stress level (σ) and net or integrated stress (S). A material's response (R) to both σ and S can be described in (Equation 1) as:

$$R = f(^{\sigma}S) = \int f(\sigma)\sigma\, dt \tag{1}$$

Degradation modes of materials can be elucidated by performing accelerated studies. A cross-correlation function can be used to predict the response observed in a system exposed to accelerated stressors compared to real-world conditions. The combination of single and multifactor tests can lead to a better understanding of the synergistic effects of stress in a real-world environment. Response is therefore a function of the convolution of multiple stressors at their service-use conditions. Murray et al. [22] exposed two grades of poly (methyl methacrylate) under two stress levels of full spectrum and ultraviolet light: a single factor accelerated test. A constant ''acceleration'' factor was not observed for key degradation modes for the two stress conditions, demonstrating that the traditional search for a single acceleration factor is unreasonable. The R(S) framework is a more versatile approach to encompass multiple stressors, stress levels and responses [22]. Mitigating these key degradation modes and lifetime penalties can increase a PV module's lifetime performance.

Predictive modeling of the power loss of PV is of important interest to the solar industry. The Sandia PV array performance model is a well established model for predicting energy production at a given location based on prescribed weather conditions. This model is designed to choose between modules and arrays at a given site or between different locations. It is commonly used by the financial community to establish project viability. It is currently not designed to determine the degradation rate of PV arrays or to quantitatively evaluate the impact of climatic stresses on a PV module's performance. This model serves as a reference for correcting PV modules' performance to standard test condition with real-world climatic data [25]–[27].

We are developing an integrated, unbiased, statistical analysis procedure to develop a predictive PV module L&DS model that will incorporate degradation modes, mechanisms and rates for PV systems in a variety of climatic zones using information from real-world and accelerated exposures and fielded materials, components and systems.

II. UL's STUDY DESIGN AND RESPONSE VARIABLES

The data used for the statistical modeling was published by E. Wang et al. [28]. Eighteen commercially available polycrystalline 60-cell solar PV modules made with fluorinated polyester (FPE) backsheets were fabricated in the same batch by DelSolar [29] and used for two accelerated exposures. Eight PV modules were subjected to damp heat aging, eight modules were exposed to UV and two modules were not exposed and instead used as control samples. Test laminates of ethylene-vinyl acetate (EVA) and glass based on a similar design as the module packaging were fabricated using the same lamination processing conditions as in the module manufacturing and were used for the interfacial adhesion tests (Peel). The edge of the test laminates were sealed with a waterproof and temperature resistant acrylic foam tape to avoid excess moisture ingress. There were no explicit variations in the PV modules used for the experiments; the intention of the work was not to analyze variations among PV modules. By using the same PV modules under two exposures conditions for the statistical analysis, there is an opportunity for a better understanding of the degradation modes present under different stressors.

A. DAMP HEAT EXPOSURE

Damp heat exposure consisted of 85 °C ambient temperature and 85% relative humidity as described in the test 10.13 of IEC 61215 Ed.2. [30]. The FPE PV modules and EVA test laminates were aged in damp heat conditions four times

longer than the IEC standard of 1000 hours. Two of the eight modules were removed from the exposure, disassembled and their packaging materials collected and tested, at every 1000 hours until the final time point of 4000 hours (Figure 1).

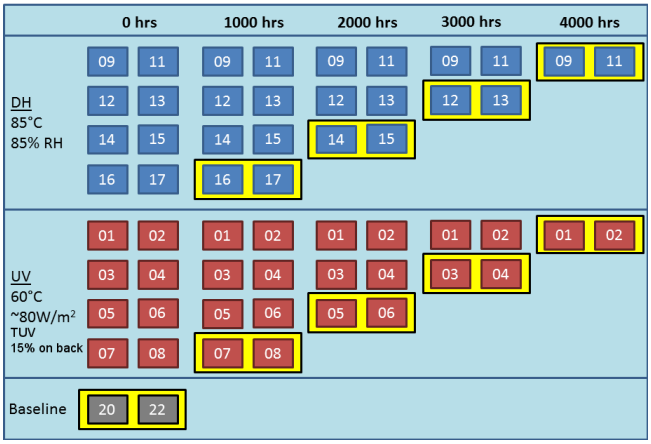

FIGURE 1. Modules harvested for each exposure condition (damp heat and UV preconditioning) showing the two modules removed at each time point. DH stands for damp heat, RH for relative humidity, and TUV for total UV.

B. UV IRRADIANCE EXPOSURE

The UV exposure was similar to the UV preconditioning test 10.10 of IEC 61215 Ed.2, [30] but with higher light intensity consisting of 80 W/m^2 ± 15% of UV irradiance from 280–385 nm plus an additional 15% of the total irradiance at the back of the PVMs and test laminates. The module temperature was controlled at 60 °C, but the relative humidity was uncontrolled. Two of the eight modules were removed from the chamber at 1000 hour increments, disassembled, and packaging materials were collected and tested until 3000 hours (Figure 1).

C. SYSTEM RESPONSES

Three system responses were measured for each of the eighteen PV modules which included peak power (*Pmax*), fill factor (*FF*) and wet insulation resistance (*WetIns*). The system level responses were measured every 500 hours for both the damp heat and UV exposures from 0-2500 hours and then these responses were measured every 250 hours from 2500 to 4000 hours for damp heat and 2500 to 4250 hours for UV experiments. *Pmax* is the peak power of a photovoltaic module determined by measuring current and voltage while varying resistance under defined illumination. The power reduction is driven by reduced FF and increased series resistance. These reductions are initially interpreted as corrosion taking place at the electrical interconnects [31]–[33]. Wet insulation resistance testing according to IEC 61215 [30] is intended to verify that the packaging materials of the PV module have insulation high enough to mitigate the risk of fire and electric hazards, even when the module is wet.

D. UNIT EXPERIMENTS

Eleven unit experiments were performed on the modules and one unit experiment was performed on the test laminates, under two exposure conditions (damp heat and UV). These experiments can be broken into performance [(Peel strength (*Peel*), glass transition temperature (T_g), water vapor transmission rate (*WVTR*), modulus (*Modu*), and differential scanning calorimetry (*DSC*)] and mechanistic categories [acetic acid content (*Hac*), thermo gravimetric analysis of EVA (*TGA*), hydrolysis of EVA (*IREVA*, *IR*2), and hydrolysis of PET (*IRBS*1, *IRBS*2)]. The unit experiments were performed every 1000 hours of testing.

1) PERFORMANCE EXPERIMENTS

Delamination is an important failure mechanism of PV modules [34]–[37]. Peel strength (*Peel*) of polymeric encapsulants such as EVA to the glass substrates of PV modules is an important factor that can affect delamination [36], [38]. The test laminates were used for the 90° peel strength measurement between EVA and glass as a function of aging time because this test could not be performed on entire modules. With dynamic mechanical analysis (DMA), the elastic modulus (*Modu*) can be measured as a function of temperature, which gives information about the material stiffness and thermal transitions like glass transition, melting or softening of the material. The storage modulus is related to stiffness and the loss of modulus to damping and energy dissipation. A significant change in the modulus could cause delamination, an inability to catch mismatches in the thermal expansion, and cracking of the cell or wiring [39], [40]. The glass transition temperature (T_g) is often measured by differential scanning calorimetry (DSC), but the DMA technique is more sensitive and yields more easily interpreted data [41]. T_g of polymers may increase with increased cross-linking [42]. Moisture ingress can occur along the edges (either along interfaces or though the edge seal/encapsulant) or through the backsheet material. High moisture transfer rates in a PV module may result in more water available for corrosion which could result in higher corrosion rates and decreased module performance [43]–[45]. *WVTR* experiment was performed to construct weight gain profiles due to moisture ingress of backsheets when stored at 40 °C/90% relative humidity. DSC is a thermal analysis technique which measures the temperature and heat flow associated with transitions in materials as a function of temperature and time. Such measurements provide quantitative and qualitative information about physical and chemical changes that include endothermic/exothermic processes or changes in heat capacity and the degree of crystallinity.

2) MECHANISTIC RESPONSES

The thermal properties of the encapsulation materials were investigated by thermo gravimetric analysis (*TGA*). The mass decrease of the sample was monitored during the heating process in dependence of the temperature. The decomposition of EVA as evidenced by the loss of acetate side groups can

be detected. Hydrolysis of acetate side groups in EVA results in generated acetic acid (*Hac*) that can accelerate the corrosion of electrical interconnects and attack the transparency coating of the cells, resulting in the eventual reduction in module performance [46]. The concentration of free acetic acid was evaluated by pyrolysis GC-MS on EVA encapsulant samples harvested from full sized PV modules (Figure 2(a)).

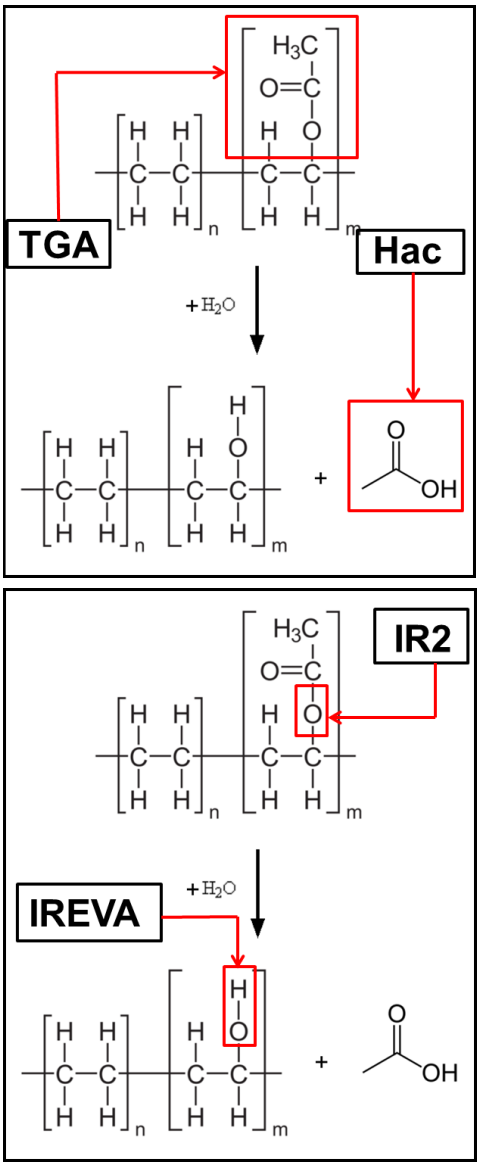

FIGURE 2. Encapsulant degradation of EVA hydrolysis. (a): The mass decrease [48] of the sample was monitored during the heating process in dependence of the temperature. The decomposition of EVA and the appearance of acetic acid can be detected. Hydrolysis of vinyl-acetate monomers in EVA results in the generation of acetic acid [49]. (b): As the exposure time increases, the acetate C=O (1735 cm^{-1}) peak decreases continuously, whereas the aldehyde/ketone C=O (1716 cm^{-1}) and O-H (near 3400 cm^{-1}) peaks increase. This results from decomposition of vinyl acetate in the EVA and the formation of aldehydes, ketones and alcohols [50]. Ester ether C-O-C /overall CH absorbance ratios were calculated to measure the relative acetate content [47].

The molecular level characterization of materials was investigated by Fourier transform infrared (FTIR) spectroscopy in attenuated total reflection mode (ATR). As the exposure time increases, the acetate C=O (1735 cm^{-1}) peak decreases continuously, whereas the aldehyde/ketone C=O (1716 cm^{-1}) and O-H (near 3400 cm^{-1}) peaks increase. This indicates decomposition of vinyl acetate in the EVA and the formation of aldehydes, ketones and alcohols during this process (*IREVA*). The *IR*2 variable was determined by the ratio 1242 cm^{-1}/2850 cm^{-1}, ester ether C-O-C /overall CH absorbance to measure the relative acetate content (Figure 2(b)) [47].

Backsheets are one of the most important module packaging components, which provide electrical insulation, environmental protection and structural support. Failure (embrittlement) of poly(ethylene terephthalate) (PET) film (a layer within the FPE backsheet) occurs when more than 0.55% of the film has hydrolyzed. The peak at 3373 cm^{-1} refers to a stretching vibration of hydroxyl groups which is related to hydrolysis (IRBS1). The changes in the stretching vibration region of methylene group (CH_2) at 2927 cm^{-1} are attributed to chain scission due to hydrolysis (IRBS2) (Figure 3) [51], [52].

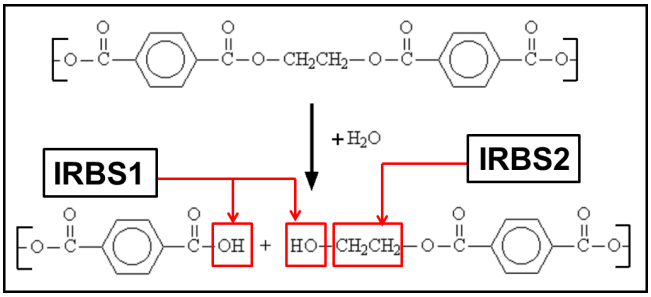

FIGURE 3. An IR peak at 3373 cm^{-1} refers to a stretching vibration of hydroxyl groups which are related to hydrolysis [51]. The changes in the stretching vibration region of methylene group (CH_2) at 2927 cm^{-1} are attributed to chain scission due to hydrolysis [52].

E. MEASUREMENT UNCERTAINTIES

The system level measurements (*Pmax*, *FF*, *WetIns*) were conducted by a PV test lab in compliance with IEC 61215 Certification Body Test Laboratory. The uncertainties of these measurements depends on the accuracy of the measuring procedures. The uncertainty of the *TGA* determination is a few tenths of a percent. This practical limitation comes from a number of error sources: sample inhomogeneity, adsorption or desorption of moisture during sample preparation and uncertainty in the *TGA* baseline. *WVTR* uncertainty depends on the accuracy of measurement procedures and sample morphology. Balance sensitivity, recording time, dryness of anhydrous calcium chloride and uniformity of thickness and flatness of the sample specimens can affect the results. The major uncertainty of acetic acid measurement (*Hac*) was from the sampling procedure. The volatile acetic acid evaporates rapidly out of the sample at room temperature; as some amount of the molecule escapes during the sample collection and processing, this increases the measurement uncertainty. Calibration of the *DSC* instrument has a significant impact

on uncertainty. In order to define the temperature scale and to fix the ordinate so it refers to known heat flow rates, it is necessary to calibrate with certified materials in the range of interest. The major contributor to the uncertainty in the peel strength (*Peel*) measurements is due to sample coupon uniformity. The sample coupons went through the same lamination process as the modules; however, their down-sizing produced mechanical stresses resulting from material thermal expansion, which may reduce uniformity of interlayer adhesion and affect the peel test results [53]. ATR-FTIR spectra measurements (*IREVA*, *IR*2, *IRBS*1 and *IRBS*2) can exhibit shifts in peak position and/or distortion of absorption band shapes when compared with transmission measurements. The use of ratios of integrated absorption bands has been shown to be an appropriate strategy for making quantitative comparisons [47]. The uncertainty of modulus and T_g measurements may be from the uniformity of the curing degree of EVA since the viscoelastic behavior is largely dependent on the degree of cross-linking of EVA [54]. The rank order measurement uncertainties were used as part of domain knowledge for initial variable selection.

III. L&DS ANALYTICS APPLIED TO THE PVM L&DS: METHODS

The statistical analysis was performed using R and Rstudio, an open source software for statistical analysis [55]. The open source nature of the data analysis and model development allows for reproducible open data science.

A. STATISTICAL AND DOMAIN ANALYTICS: L&DS ANALYTICS

A PVM L&DS model can provide knowledge of rank ordered degradation modes for different climatic zones and stress conditions, which can highlight modes contributing to performance and lifetime for a particular use condition. A statistically valid approach is necessary for the development of a reliable PVM L&DS model for reasonable lifetime prediction.

Structural equation modeling (SEM) allows for confirmatory and exploratory modeling and facilitates the generation of a system of equations describing the relationships between variables in a model. The statistical analysis for a PVM L&DS model requires many measurements or a large sample size if the number of candidate predictors is large, [56]–[58]. In addition, the standard SEM software typically only fits a system of linear equations, and a completely domain-independent SEM model selection by a χ^2-type measure may be misleading [57]. Thus, our approach is a *domain semi-supervised "generalized system equation modeling"* (*semi-gSEM*), which can allow nonlinear relationship among variables. The *semi-gSEM* approach has the following 4 steps (Figure 4):

Basic Steps of L&DS Analytics

1) system-level components are selected by both statistical evidence and domain knowledge;
2) path directions and the best fit functional relations between each pair of the components (or variables) are determined from a set of linear and nonlinear functions, which includes functions with change points to allow changes in the degradation rates;
3) the resulting overall system with detailed paths and fitted relationships is examined again by statistical diagnostics;
4) if an update is signaled from step 3, "offending" parts in step 2 will be refit and then step 3 repeated until there is no such need.

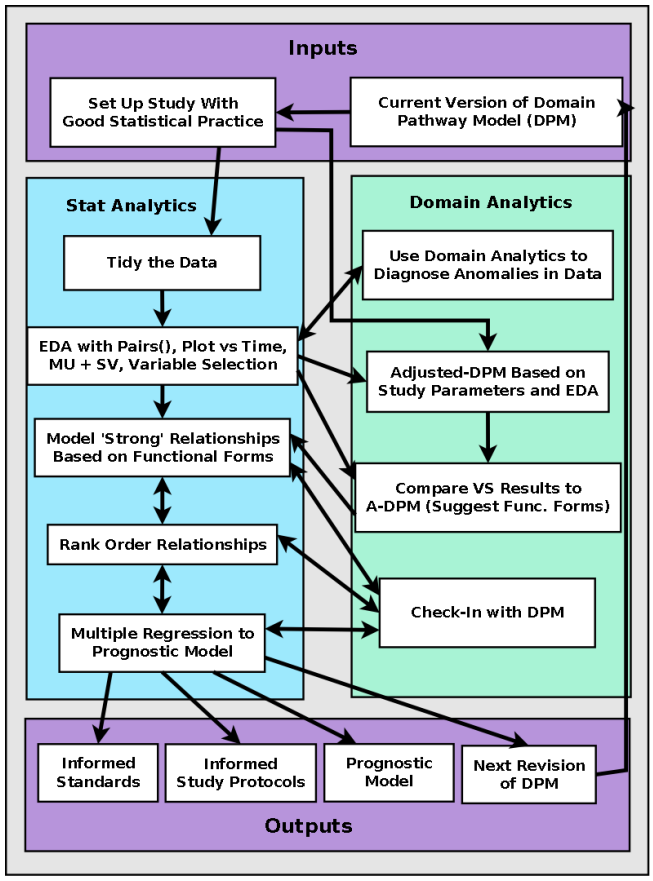

FIGURE 4. Iterative *semi-gSEM* procedure for the PVM L&DS model. MU is measurement uncertainty. SV is sample variability. EDA is exploratory data analysis. A-DPM is the adjusted domain pathway model.

Statistically significant relationships (SSRs) are used to analyze different degradation modes, responses and pathways under the influence of contrasting stressors. Metrics such as Akaike information criterion (AIC) [57], R^2 [59], [60], adjusted R^2, or predictive R^2 and P-values [59], [60] should be used together to gauge the strength of derived relationships between variables and ultimately their impact on degradation and performance loss. The set of candidate functions mentioned in Step 2 will be chosen based on domain knowledge from physics and chemistry and checked with exploratory data analysis in statistics. Since we use domain knowledge to set a preliminary set of variables and decide the parametric

functional relations for consideration, there will not be an issue of overfitting or inconsistency in some nonparametric maximum likelihood estimation procedures. After statistical analysis is performed, then domain knowledge is used to validate and understand the correlations and results. Observations can be framed in terms of known mechanisms and pathways as well as a particular system response. SEM allows for random, measurement, systematic and method errors to be incorporated into the model removing particular bias from the resulting model [61].

Domain knowledge can be used to identify the probable active and quiescent pathways. Different pathways can be activated by different stressors or stress levels and need to be incorporated into the PVM L&DS model. Figure 5 shows some example PV module degradation pathways which are based on observations from both real-world and accelerated exposed modules [25], [26], [34], [62]–[66]. When module failure modes can be attributed to processes that are only activated under accelerated exposure conditions or accelerated exposure conditions are chosen that fail to activate pathways observed in real-world exposed modules, it signals inappropriate testing conditions that provide little insight on module performance in the real world. To assess which exposure conditions recreate sensible real-world module degradation world module degradation modes for the prediction of PV module performance, the deciding factor will be which degradation pathways are activated by the chosen stress levels using the R(S) framework and L&DS [22].

The iterative nature of the PVM L&DS model allows for continuous refinement as more knowledge is gained through accelerated exposure studies, fielded module studies from real-world exposures and new technology insertion. The correlations and predictions will become stronger over time; therefore producing a predictive, statistically significant prognostic model. Proper documentation of the limitations and scope of a predictive model is important to ensure that a model is providing useful information on the projected lifetime of the system under observation [67]. In addition, this PVM L&DS model contributes to reproducible open data science.

B. DATA CLEANING AND MUNGING

The data requires tidying before it can be subjected to analysis. This data preprocessing is important in any data analysis. Here, it entails arranging the data into a predefined data structure that features approximately coincident observations on equivalent systems described in terms of multiple variables. Once arranged in this way, exploratory data analysis is used to search for inconsistencies and decide a preliminary set of variables that are to be statistically examined using Principle 1 or 2 below for their inclusion as important system components. Care must be taken to appropriately handle outliers and missing data so that they do not interfere with the analysis. In this specific case, missing values were re-measured on retained samples and variables where significant outliers representing measurement or recording error were found were omitted from the analysis.

Prior to incorporating variables into the analysis, contributions to the uncertainty of the values by both sample and measurement variability is quantified and related back to domain knowledge. This assists in cases where choices must be made between variables, as it is best to include variables with lower uncertainty. Additionally, the *Time* variable should be renormalized to a similar scale as the measurements, to avoid numerical and computational error issues due to mismatch in the magnitude of the numbers. This data preprocessing experience will be extremely useful in developing study protocols in the future.

C. MAP TO DOMAIN KNOWLEDGE

The models relating each variable to *Time* must be checked via domain knowledge for consistency to the phenomena being measured. Chemical and physical processes are typically linear and exponential, so if a polynomial model is found to provide the best fit, it could indicate that there are change points signaling the influence of combined effects, such as an acceleration in the degradation rate. Additionally, phenomena anticipated to be exponential could appear linear if test conditions are not aggressive enough to elicit sufficient response over the total measurement time. Every

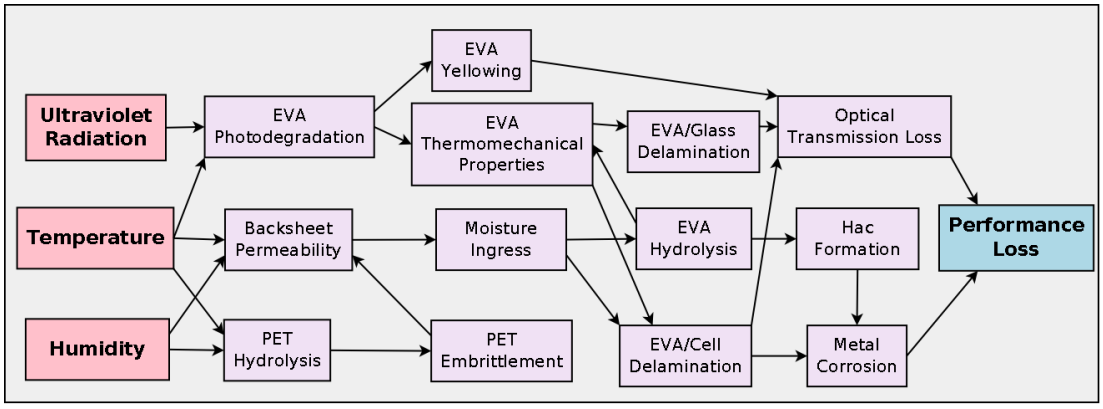

FIGURE 5. Example PV module performance degradation pathways informed by domain analytics. The left red boxes show stress variables. The right pink box is a system response variable and the purple boxes represent unit response variables.

model, SSR or ranking of variables needs to be confirmed with what is known in the literature and what is known to be possible within physical and chemical domain expertise. Domain analytics from literature and observed experience are then applied to the models to identify all the degradation modes and pathways and to determine whether degradation is occurring in a simultaneous or sequential fashion with saturation, accumulation or runaway genesis of degradation products. Domain knowledge is necessary in generating a comprehensive L&DS framework.

D. VARIABLE IDENTIFICATION

In a typical data analysis problem, there are candidate predictors and response variables. Often, some predictors have little or no further influence on the response variable given the presence of other predictors. The procedure to identify those predictors or to select the ''best'' subset of the predictors, such that the statistical model based on this subset of predictors is comparative to the full model based on all the predictors, is called variable selection. In this analysis, there are a small number of observations and a large selection of variables. Due to the limited data, domain knowledge has been used to aid the selection of a subset of predictors to construct the SSR models.

E. VARIABLE TRANSFORMATIONS AND FUNCTIONAL FORMS

In cases where the scales of the values are magnitudes apart, a transformation of one or both of the variables may be necessary to avoid numerical computational errors such as significant digit cancellation. Care must be taken that variable transformations are consistent for all explored variable relationships, so that the results of statistical analysis remain comparable. This is desirable for the purposes of testing the strength of the proposed relationship, in terms of how closely the observed measurements correspond to the physical phenomena indicated theoretically by domain knowledge. In order to evaluate this, the data values are fit to known functional forms chosen based on exploratory data analysis and domain knowledge of chemistry and physics. The functional forms considered for the variable fits were constrained to linear, quadratic, simple quadratic, exponential, logarithmic, nonlinear least squares (nls) [68] and change point with simple linear functional forms on either side of the change point (Table 1). A combination of the R^2, adjusted-R^2, and predictive R^2 value are used to evaluate each model for its goodness-of-fit and determine if a model is appropriate for describing the data in a way that supports the underlying theory.

TABLE 1. The variable fits explored in our *semi-gSEM*.

Variable Fits	Functional Form
Simple Linear (A)	$y = a + bx + \varepsilon$
Quadratic (B)	$y = a + bx + c * x^2 + \varepsilon$
Simple Quadratic (C)	$y = a + c * x^2 + \varepsilon$
Exponential (D)	$y = a + d * \exp^x + \varepsilon$
Logarithmic (E)	$y = a + f * (\log(x)) + \varepsilon$
Linear Change Point (F)	$a + d * (1 \pm \exp(g(x - h)) + \varepsilon$
Nonlinearizable Exponential (G-up, H-down)	$y = a + b * x + b_1 * (x - c)_+ + \varepsilon$

F. PRINCIPLES OF VARIABLE SELECTION AND RANKING

The number of variables considered in the statistical analysis should not be bigger than $n-2$, where n represents the number of observations. In this case $n = 8$ observations, meaning at most six variables from the set of unit experiments and *Time* can be included in the SSR pathway models; therefore, variables to be included in the model determination must be chosen on the basis of measurement confidence and domain knowledge-based expectation of significance to the overall model.

The objective for this L&DS analytics development is to determine a methodology to find reasonable predictive pathway models instead of a complete causal diagram. Ideally, the PVM L&DS model will include an overall, complete causal diagram or relationship network that links all possible relationships from covariates (denoted by $x = (x_1, \ldots, x_p)$) to the response variable (denoted by y) and among these covariates. The overall optimal model requires an optimization of all possible models, for which there is not a uniformly optimal procedure [57], [58]. Therefore, an iterative approach is used for our SSR Identification Procedure:

1) Find the first level relationships from x to y, using Principle 1, or 2 below, statistically.
2) For each significant x included in Step 1, treat it as new variable y, and the remaining x's as new x's and then repeat Step 1 on new x and new y.
3) In the process of Step 1 and Step 2, we remove or investigate any estimated relationship that is inconsistent to domain knowledge, even if it is significant based on data.

The two different principles, for variable selection and ranking of the variables' contributions to the system level change, may lead to the same or different SSRs and pathway diagram models. Regardless which principle or pathway, the resulting relationship described by any of the two principles should be whatever the true relationship supported by evidence/data/science is and may not necessarily be linear.

Principle 1 determines the univariate relationships in the spirit of the Markovian process [59], [60]. In this case, the relationship between each pair of system elements, including predictors and the system level response is determined with the Markovian property that assumes the value of the current predictor is sufficient in relating to the next-level variable, i.e., the relationship is independent of the specific value of the preceding-level variable to the current predictor, given the current value. The variable importance now can be measured again by the R^2, adjusted R^2 or a predictive R^2 no matter whether the relationship is

linear or not. In the resulting relationship, at least one P-value for the resulting coefficients should be small. A P-value less than 0.05 usually signals a significant contribution from the resulting model. However, sometimes, for a predictive purpose, the coefficients with P-values up to 0.1 or 0.15 may be included. Typically, the smaller the P-value, the stronger the significance of this variable, inside the current model, is. Thus, a good system should be evaluated based on R^2, adjusted R^2, or a predictive R^2 together with an examination of P-values, and ideally in addition, with some statistical diagnostic plots.

Principle 2 resembles the multiple regression principle in the way multiple predictors are considered simultaneously. Specifically, the first-level predictors to the system level variable, such as, *Time* and unit level variables, acted on the system level variable collectively by an additive model (Equation 2):

$$Pmax = f_i(time) + f_k(IR2) + \cdots + e \tag{2}$$

where f_i's are appropriate (parametric) function fits. In this case, a generalized multiple R^2 can be computed to indicate the overall strength of these variables in modeling a system level variable. In linear SEM, f_i's are linear in terms of unknown parameters. This collective additive model can be found with a generalized stepwise variable selection [69] (using the step() function in R, which performs variable selection on the basis of AIC [55]) and this proceeds iteratively as described above. The ranking of variables within each collective additive model can be based on P-values if the linear regression in Equation 2 is valid. If the relationship is not linear, the overall comparison/rank cannot be developed unless the paths are independently interpreted though they were obtained collectively using Principle 2. In this case, the ranking is then equivalent to that under Principle 1.

IV. L&DS ANALYTICS: RESULTS

Two unexposed modules were initially disassembled and unit level variable measurements taken for a shared baseline between the damp heat and UV exposures. Two additional modules were disassembled at each 1000 hour interval (up to 4000 hours for the damp heat exposure and 3000 hours for the UV exposure) for measurements of the unit level variables. Though the system level variables (*Pmax, FF, WetIns*) were measured more frequently than 1000 hour intervals, they share only these time points with the unit level variable measurements. These coincident observations allow comparison between measurements of different variables from identical modules.

The number of measurements at each time point for each variable is not consistent. Some variables were measured multiple times (2-6) per disassembled module at each time point, while others were only measured once. Additionally, individual measurements at identical time points between different variables are only comparable to one another on the basis of their sample origin (which module they came from), and do not correspond directly to one another even if the number of measurements is identical. Therefore, in the event of multiple measurements of a single variable from a single module at a single time point, the measurements were averaged to a single value to enable a system wide comparison.

Variables differ slightly in regards to how the results of the measurements are interpreted into discrete values. The results of $Pmax$, FF, $WetIns$, $WVTR$, Hac, $Peel$ and T_g gave a single value which can be used without modification. The test results of $IREVA$, $IR2$, $IRBS1$ and $IRBS2$ are spectra, which are interpreted into specific meaningful ratios of integrated absorption bands to provide singular values. The *TGA* test provides a curve of sample weight vs temperature, a portion of which (characterized by changes in the slope of the curve) corresponds to losses of specific polymer side groups. The total weight lost over this interval corresponds to the amount of the side groups present in the polymer, which functions as a single discrete value for each *TGA* curve. The DSC test provides a curve describing the change of heat flow into a sample over a scanned temperature range. Changes in the heat flow correspond to changes in the degree of crystallinity present in the sample. The degree of crystallinity can be quantified, which functions as a single discrete value for each DSC curve. Dynamic mechanical analysis (*Modu*) results in a curve describing changes in material modulus over a scanned temperature range. A single temperature was chosen (71.363 °C) , and the modulus at that point used to describe each dynamic mechanical analysis curve as a single discrete value.

Four pairs of two coincident observations were used in the SSR development: for 0-3000 hrs, with data from two modules at each time point for a total of sixteen data points for each variable for both damp heat and UV experiments. There were a total of fourteen modules for both of the experiments because the baseline data shares the same module origins for both experiments. To build a system wide pathway at each level, statistically only six variables can be used in the model development because there are only eight coincident observations. These six variables must include *Time* because the *Time* variable is being used as a proxy for exposure since stress intensity is constant and therefore net stress scales with time. To overcome the limitations of the eight coincident observations, both exploratory data analysis (based on pairwise plots of all variables) and domain knowledge were then used to identify system and unit level variables and differentiate the unit level variables to mechanistic or performance variables. The model development was performed for two of the system level variables ($Pmax$, FF). Domain knowledge was also used to determine if unit level variables were related to the same degradation modes. The data for each of the variables was investigated to determine if the data was sensible and to determine the impact of the measurement uncertainty and sample variability on the variable data. However, once the system wide pathway is set, the individual relationship between a pair of variables is built based on all the available points, ensuring a more reliable relationship.

The functional forms considered for the variables were constrained to linear, quadratic, simple quadratic, exponential, logarithmic and change, nonlinear least squares (nls) and change point with simple linear functional forms on either side of the change point. The specific change point in the change point fits was determined using the damp heat *Pmax* variable related to *Time*. This was not done with UV because there was not enough of a change in the slope for the UV experiment. For the variable transformations, the linear change point was determined to be at 1890 hrs or 2.6 months, which gave the highest R^2 value for the transformation of *Pmax* with damp heat exposure (Figure 6). This set of candidate models is chosen based on exploratory data analysis and domain knowledge.

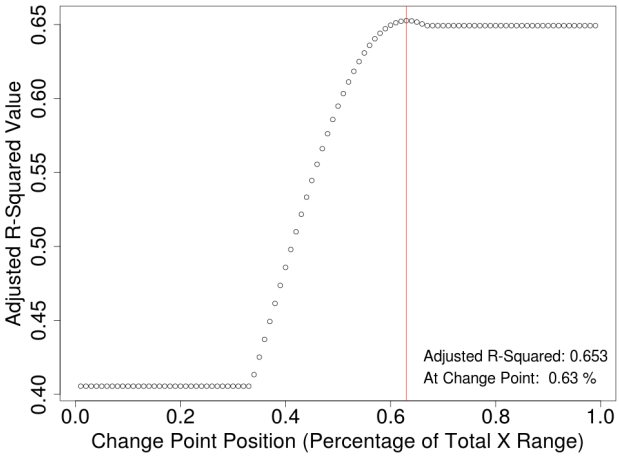

FIGURE 6. The linear change point was determined to be 1890 hrs for *Pmax* with the damp heat exposure.

A. RANK ORDER OF UNCERTAINTIES

The rank order of the measurement accuracy of each variable is useful for selecting variables to include in the model selection process, but this was not directly done in the current analysis. Rather, the rank order of measurement uncertainties was used when applying domain knowledge to decide which variables should be used in the models as the initial number of variables was limited due to the limited number of sets of coincident observations.

B. VARIABLES

For both damp heat and UV, the system level responses were *Pmax*, *FF*, and *WetIns*. The unit level predictors considered for damp heat were *Peel*, *Hac*, *TGA*, *Modu*, T_g, *DSC*, *IREVA*, *IRBS*1, *IRBS*2, and *IR*2. In addition to all the unit level predictors considered for damp heat, the unit level predictors considered for UV also included *WVTR*. After limiting this initially considered pool of variables based upon domain knowledge and measurement confidence, the variables included in the model selection process were *Pmax* or *FF*, *Hac* or *TGA*, *IREVA* or *IR*2, *IRBS*1 or *IRBS*2 and *Time*. For each variable involved in a specific model representing a combination of variables with an associated test condition, there were eight observations.

C. DATA STRUCTURES

The data structures for damp heat and UV were very similar except there was an additional unit level predictor considered for UV, *WVTR*. For both system and unit level variables, there were eight measurements for each variable at time points ranging from 0 to 3000 hours. The measurements were observed at 0, 1000, 2000 and 3000 hours and there were two measurements at each time point.

D. STATISTICALLY SIGNIFICANT RELATIONSHIPS (SSRs)

Principle 1 was used to find SSRs between combinations of variables under both damp heat and UV exposure conditions. The specific case of the relationships between the variables *Time*, *Hac*, *IR*2 and *IRBS*1 and *Pmax* are shown in Figure 7 and Figure 8. The results are markedly different between the two exposure conditions, which indicates differences in the active degradation mechanisms within the systems under the influence of different stressors. Relationships with an adjusted R^2 value below 0.2 were omitted from the SSR models. The boxes around each relationship in the figures show four varying degrees of border thickness based on the strength of the R^2 value where R1 has the thinnest border (0.2-0.5), R2 (0.5-0.7), R3 (0.7-0.9) and R4 the thickest ($\geq$ 0.9). P-values correspond to the significance of the parameters in the model. for example, in an exponential model: $f(x) = a_1(1 - e^{a_2(x-a_3)})$, the P-values are for the significance of H_i: $a_i = 0$ vs. $H_i = a_i \neq 0$, for $i = 1, 2, 3$, respectively.

1) DAMP HEAT AND UV SSRs

The damp heat exposure showed a strong change in *Pmax* with *Time* (Figure 9(a)), while the UV exposure did not show a significant change in the *Pmax* values (Figure 9(b)). The damp heat exposure results show very strong R^2 values for many of the "best" fitting models using Principle 1. The model with the most SSRs was using *Time*, *Hac*, *IR*2 and *IRBS*1 for the system response of *Pmax* (Figure 7). The UV exposure condition results show mediocre R^2 values for many of the "best fitting" models. The model with the most SSRs was using *Time*, *Hac*, *IR*2 and *IRBS*1 for the system response of *Pmax* (Figure 8).

V. DISCUSSION

A. METHOD

Domain-semi-supervised gSEM procedure used Principle 1 and 2 to quantitatively evaluate the SSRs between variables to elucidate the information content of the different unit variables on a system variable. The *semi-gSEM* allowed for functional forms that were determined through domain analytics to be used as variable fits. A resulting generalized system of equations will result from further iterations of the *semi-gSEM* procedure that will be used for the predictive PVM L&DS model.

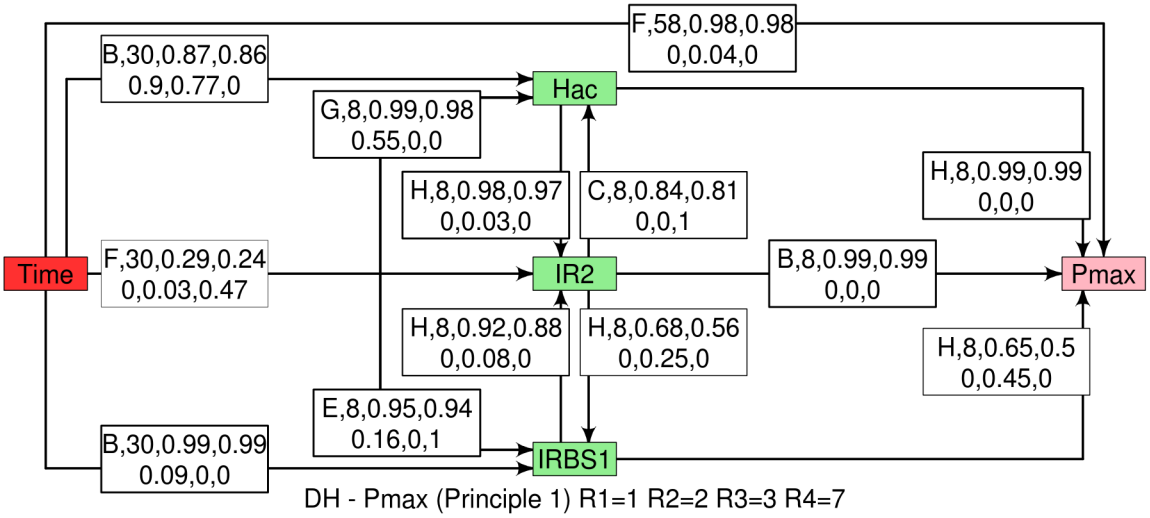

FIGURE 7. Model generated with the most relationships shown for Principle 1 for the damp heat exposure for the system response of *Pmax* using the unit variables of *Hac*, *IR*2 and *IRBS*1 shows 13 relationships. Information on each relationship is described in the box. The information contained is functional form, number of observations, R^2, adjusted R^2, P-value 1, P-value 2 and P-value 3, respectively. The strength of the SSR is summarized by the line width of the SSR border based on the R^2 value to aide visualization (below 0.2 not shown, R1 has the thinnest border (0.2-0.5), R2 (0.5-0.7), R3 (0.7-0.9) and R4 the thickest ($\geq$ 0.9)). The functional forms are designated as A (simple linear), B (quadratic), C (simple quadratic), D (exponential), E (logarithmic), F (linear change point), G (nonlinearizable exponential-up) and H (nonlinearizable exponential-down).

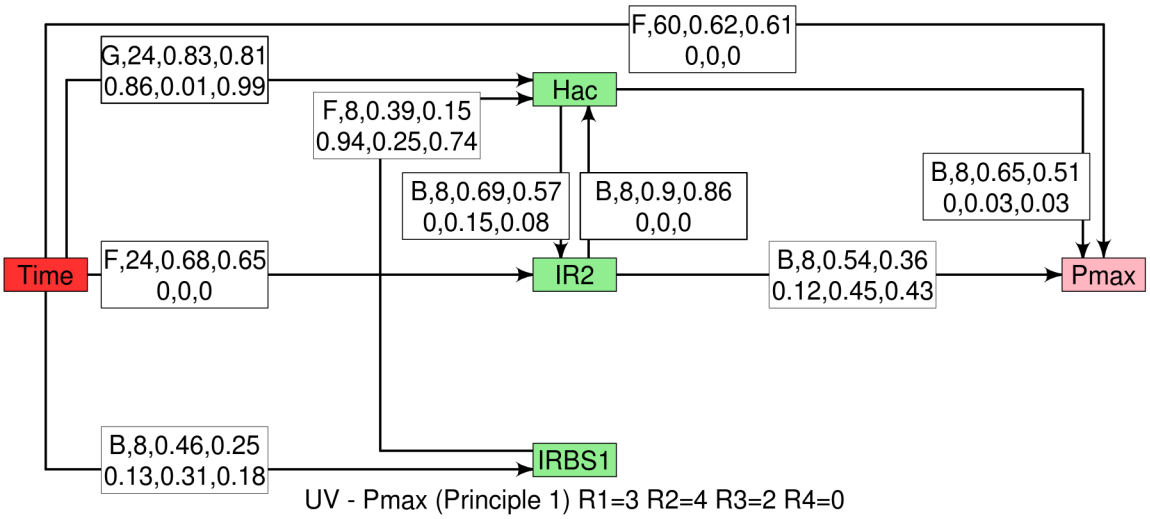

FIGURE 8. Model generated with the most relationships shown for Principle 1 for the UV exposure for the system response of *Pmax* using the unit variables of *Hac*, *IR*2 and *IRBS*1 shows 10 relationships. Information on each relationship is described in the box. The information contained is functional form, number of observations, R^2, adjusted R^2, P-value 1, P-value 2 and P-value 3, respectively. The strength of the SSR is summarized by the line width of the SSR border based on the R^2 value to aide visualization (below 0.2 not shown, R1 has the thinnest border (0.2-0.5), R2 (0.5-0.7), R3 (0.7-0.9) and R4 the thickest ($\geq$ 0.9)). The functional forms are designated as A (simple linear), B (quadratic), C (simple quadratic), D (exponential), E (logarithmic), F (linear change point), G (nonlinearizable exponential-up) and H (nonlinearizable exponential-down).

B. INFORMED EXPOSURE AND EVALUATION PROTOCOLS

In order for accurate statistical analysis to be performed, accelerated and real-world experiments need to be structured to give a significant number of coincident observations or at least approximately coincident or comparable observations. In order for these types of tests to be worthwhile and provide

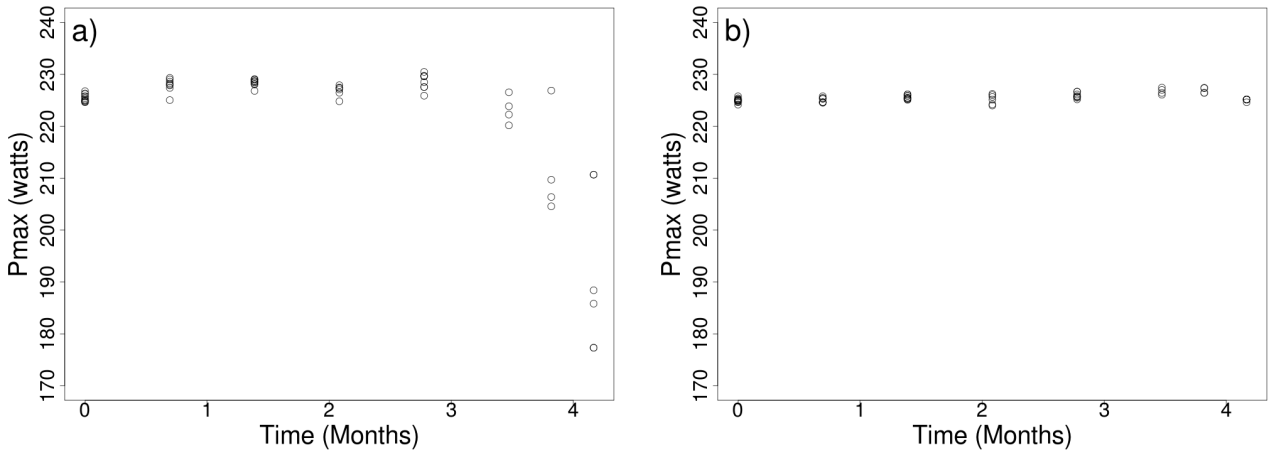

FIGURE 9. (a): *Pmax* data for the damp heat experiment (b): *Pmax* data for the UV experiment [28]. Each circle describes a measurement on a module. The *Pmax* was measured for each of the modules at each time point.

the highest information content for the PVM L&DS analytics, the experiments need to be strategically constructed and executed. The data used in this analysis were averaged; however, it is more robust to use all the data available even for the system level model building. Therefore, further iterations and development of the statistical analysis for the PVM L&DS model will use all possible data points for a more statistically accurate model development.

Important information content can be extracted from this data set about accelerated exposure design for a statistically relevant data set. It is necessary to have a large enough sampling at time points throughout the experiment. In the case of this data set, having time points at every 300 hours would allow for a more comprehensive model to fit the data. In addition change points can be more easily elucidated when data is collected at more time points early on in the experiment because the change between the linear and exponential responses can be more clearly seen.

1) VARIABLES AND COINCIDENT OBSERVATIONS

As mentioned previously, the number of coincident observations of each experiment is very important in order to be able to understand SSRs and to model all the variables. The number of coincident observations needs to be large enough to not limit the model development. This allows for the relationships between the system level responses and the unit experiments to be elucidated. In the case of data analyzed here, the number of observations was small which necessitated the use of domain knowledge to determine which variables should be used in the initial modeling of SSRs; therefore, a completely data driven approach was not possible to explore the data.

Samples should be measured more than once at single time points in order to gain an understanding of the sample variability and standard deviation. Characterizing the sample variability of each type of measurement allows the actual degradation trends to be elucidated so that the model will not be based on noise or possible outliers due to an instrument, measurement or manufacturing error.

Structuring evaluations so that there are multiple experiments showing a single degradation mode or several measurements along a degradation pathway (precursors, reactants, byproducts, products) can provide additional information about the degradation pathway and its relationship to other variables. More than one experiment was performed in order to understand mechanistic responses such as the experiments to determine acetic acid production. For acetic acid production several different variables were measured which can be used to elucidate information about the degradation pathway that yields acetic acid. Variables that measure the exact same product of the degradation pathway cannot be included in the same model without resulting in collinearity of the model, but they can be interchanged in the model development. This also allows variables with the least measurement and sample uncertainty to be included for the best model development.

Some variables will have no significant relationship to the system level response because the degradation response of that material or component does not directly affect the system level response, it is a very minor contributor or the degradation of that material was not enough to cause a change. Some variables are highly correlated with others, and hence are redundant variables in an analysis under Principle 2. This is an especially important phenomenon to be aware of, which may be highlighted in the differences observed between models developed from systems under different exposure conditions such as the UV exposure.

2) UNBIASED ANALYSIS

It is necessary to do the analysis with a standard set of variables so that the statistical model development is not prebiased. For these results, the number of variables was more than the $n - 2$ number of degrees of freedom making it necessary to choose between the variables for analysis using

domain knowledge. A study can be structured in a way that the number of unknown parameters or coefficients is large compared to the number of variables so that all the variables can be included in model development and investigated to determine statistically significant relationships among the variables. A study can either increase the time or the time points over which data is collected (e.g., every 300 hours instead of 1000 hours, or go to 7200 hours instead of 4000 hours), can increase the sample size (e.g., four samples at each time point instead of two), or do both of these things to increase the quality of statistics for model development. In the case of this analysis, the small data set constrains the model development to considering variables pre-chosen with domain knowledge prior to the statistical analysis.

C. L&DS

1) STATISTICAL ANALYSIS GUIDED BY DOMAIN KNOWLEDGE

Domain knowledge was used to reduce the number of variables to be incorporated into the SSR and pathway diagram. Due to the number of coincident observations in the data set (8), at most six variables could be included into the SSR and pathway diagram. Measurement uncertainty in the data and sample variation, in combination with domain knowledge, can be used to determine whether a particular measurement might be a better candidate for inclusion. All relationships found to be statistically significant are also checked against domain knowledge, and are only to be included in the final model if they correspond to known mechanistic responses. This allows for all possible relationships to be identified, while removing those that are not expected to be beneficial to the predictive capacity of the final system of equations.

2) VARIABLES REMOVED FROM MODEL DEVELOPMENT WITH DOMAIN KNOWLEDGE

The final set of unit level variables retained for the model development procedure were all mechanistic in nature, which reflects the desire to discover specific characterizable degradation pathways within the system. Non-mechanistic measurements could still conceivably be useful as a proxy for suspected mechanisms contained within them, but in the case of these experiments, the following variables were considered suspicious with regards to their information content. *Peel* was excluded from the analysis on the basis of relatedness to the system under observation. The measurements were prevented from being coincident observations because the variable was measured on test laminates instead of the modules themselves. This introduced major uncertainties into the measurements, due to the non-optimized laminating conditions for the comparatively smaller test coupons. *WVTR* was excluded from the analysis due to missing measurement values. It was impossible to measure the *WVTR* of the module backsheets for modules exposed to damp heat conditions past the 2000 hour mark, where the components were too brittle to be harvested. *Modu*, T_g and *DSC* results were all excluded from the analysis because they all indicate complex phenomenon which are difficult to attribute to a single mechanism of action. This, combined with some uncertainty in interpretation of the raw data values, made these variables very unlikely to add any predictive capacity to a final model. The two system level variables retained for the model development procedure were *FF* and *Pmax*. *WetIns* was not included as a system level variable in the analysis, due to prominent outliers in the data, which could not be removed without reducing the number of observations below acceptable limits.

3) MODEL DEVELOPMENT

In this analysis, the data was fitted with six functional forms corresponding to known mechanistic responses. For the purposes of investigating the presence of change point effects corresponding to damage accumulation, one of these functional forms includes a change point with two simple linear functional forms on either side. In the future a more appropriate fit will be performed for the PVM L&DS model with a larger number of observations. Typical chemical and physical processes are either linear or exponential responses. Quadratic responses aren't a commonly characteristic of these processes. Therefore, if a variable transformation appears to be quadratic, it can be an indication of a change point in a process.

In accordance to Principle 1, the best fitting models for relationships between variables were chosen from these six functional forms, and the variables' impacts on other variables were ranked based on the R^2 of the corresponding best functional fit. This is an appropriate and reasonable method because the ranking is constrained to a class of functional fits. The R^2 is based on the fit so if the fit is poor or over fitted this could be reason to question the model.

The averaging of the values to meet the requirement of coincident observations reduces the information contained in the data, but in order to develop a statistically significant model this was required for the unit level experiments, where uneven numbers of multiple measurements on identical samples at identical time points prevented individual measurements from being directly comparable to one another. This was not the case for the measurements' comparability to *Time*, where there was a direct correspondence between each measurement and the time point at which it was taken. Here all the available data points could be used without averaging, creating a larger number of observations upon which to base the model fitting of the six functional forms.

It is important to note, however, that the Markovian nature of the modeling of these univariate relationships ignores the simultaneous impact of other variables, and treats the relationship as occurring solely between the two variables in question [59], [60]. This is a major source of weakness in a technique for investigating the combined influence of multiple simultaneous and sequential degradation mechanisms, and will be addressed in future iterations. Principle 2 does not have the weakness of ignoring the simultaneous impact of the other variables; however, currently, most available

packages assume all relationships to be linear, which is not necessarily the case. Figure 7 and Figure 10 have the same variables, but are two models with different R^2 values because Principle 2 model shows the interaction of the entire system. Principle 1 makes sense at an individual level because of the nature of the single stress exposures in this experiment. The multifactor nature of the real world with interactive degradation pathways is more accurately explored by using Principle 2 (Figure 10).

4) STRESS CONDITIONS

The models using Principle 1 show interesting contrasting sets of relationships between the variables under two different environmental stress conditions. The damp heat stress condition showed a very significant change in Pmax during the exposure, which was not present in the UV exposure (Figure 9(a) and Figure 9(b)). It is important for a stress condition to be strong enough to produce a meaningful response. The relationships found in the UV exposure might not be as meaningful as those for damp heat because there was very little change in the responses, which could be attributable to the measurement uncertainty. For the UV exposure, there was no evidence that *FF* had other statistically significant relationships except to *Time* (Figure 12) compared to the relationships seen in the *FF* for the damp heat exposure (Figure 11). These relationships still may be present in a larger data set that includes more information about sample variability and measurement uncertainties. The stress conditions need to induce degradation in the system response in order to increase confidence in the SSRs and model development. The model development for Figure 11 showed the relationship from *IR*2 to *Hac* to have a reasonable R^2 value for the fit, but all the P-values were very high. The step() function was applied to this relationship and the quadratic relationship became a simple quadratic form with a reasonable R^2 and P-values.

5) EVALUATIONS

It is possible to have a very comprehensive experiment, but to perform evaluations on modules that do not provide maximal information content. Figure 8 and Figure 13 show different relationships indicated between variables that are intended to measure the same mechanism of the decomposition of vinyl acetate in EVA and backsheet degradation. *IR*2 and *IREVA* are two measurements of the EVA response that may not be a major contributor in a UV only exposure (Figure 12); however, it may be that the stress condition was not strong enough to induce a significant response. In the case of the system responses, *Pmax* shows more relationships for this data set than *FF*; therefore, the possibility that *Pmax* might be a better measurement of overall system degradation than *FF* is evidenced in this small data set.

6) EVA DEGRADATION MECHANISMS

The variables that indicate EVA degradation mechanisms are *Hac* or *TGA* and *IR*2 or *IREVA*. The variables were interchanged during the SSR pathway model development because the *semi-gSEM* procedure does not support two variables measuring the exact same response due to the risk of collinearity. *Hac* (Figure 7) showed the same number of SSRs as *TGA* (Figure 14) however there was a higher R^2 for the relationship between *Hac* and *IRBS*1 than between *TGA* and *IRBS*1, while *TGA* had a slightly higher R^2 value with *IR*2 than *Hac* and *IR*2. This indicates that *Hac* may have slightly more information content than *TGA* as a metric of investigating EVA degradation mechanisms. The initial model development for Figure 15 showed the relationship from *IRBS*1 to *TGA* to have a quadratic functional form with a good R^2 value (0.85); however, all the P-values were high which indicated that the functional form fit might not be optimal. The step() function was implemented again on that relationship (Step 4) and the functional form of a simple quadratic with a reasonable R^2 (0.52) had at least one low P-value, which suggests that this is a better fit to the data.

In the case of the damp heat exposure and *Pmax*, *IR*2 showed more SSRs with higher R^2 values (Figure 7) than the model using *IREVA* for all combinations of *Hac*, *TGA*, *IRBS*1 and *IRBS*2 (Figure 15), which indicates for these experiments that *IR*2 has more information content than *IREVA* as an indication of the EVA degradation within a module. This is also true in the case of the UV experiments and the system response of *Pmax*. The *IREVA* values were calculated with the ratio of 1242 cm^{-1}/2850 cm^{-1}, ester ether C-O-C/overall CH absorbance ratios. These are relatively strong sharp peaks and the area is easily calculated for each of these peaks. In contrast, the *IREVA* values were calculated based on the broad OH peak between 3500 and 3300 cm^{-1}. There is measurement uncertainty introduced when measuring the area of this peak due to the broad shape and low intensity.

7) BACKSHEET DEGRADATION MECHANISMS

The variables for backsheet degradation (*IRBS*1 and *IRBS*2) were interchanged in the model development. In the UV experiments and *Pmax*, *IRBS*2 showed more SSRs with higher R^2 values than for the variable *IRBS*1 for each possible combination of the EVA degradation mechanism variables (Figure 13 and Figure 16). In the damp heat exposure, *IRBS*2 showed more SSRs with higher or very similar R^2 values to models with *IRBS*1. This indicates that *IRBS*2 might be a better indicator of backsheet degradation in UV induced degradation compared to *IRBS*1, where as in damp heat they have similar information content.

8) PERFORMANCE VARIABLES

If there had been more coincident observations, the performance variables could have been included into the model development. The performance variables could be used as confirmatory for mechanistic variables in model development. Due to the low number of coincident observations, only mechanistic type variables were included.

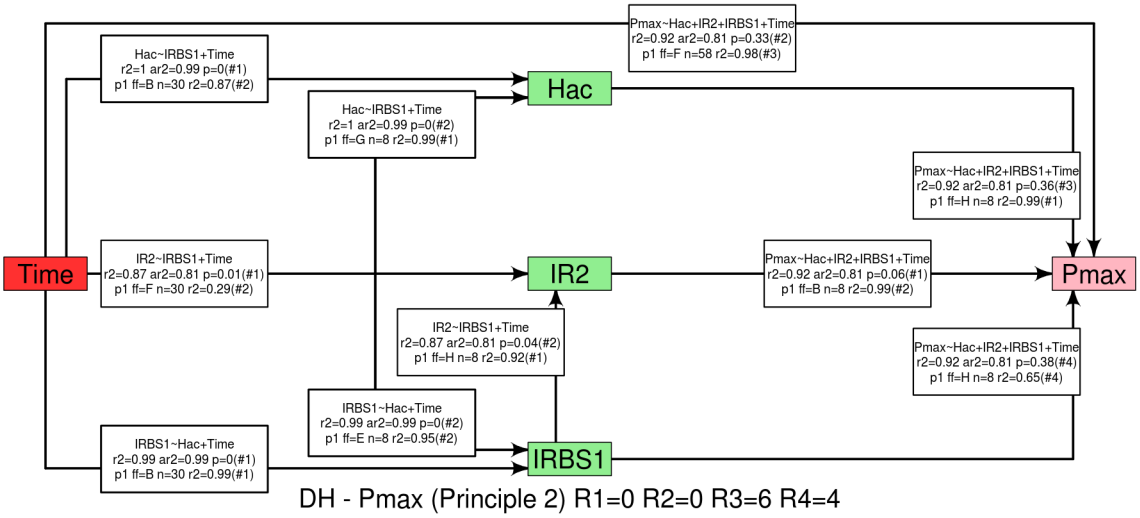

FIGURE 10. Model generated with the most relationships shown for Principle 2 for the damp heat exposure for the system response of *Pmax* using the unit variables of *Hac*, *IR*2 and *IRBS*1 shows 10 relationships. The strength of the SSR is summarized by the line width of the SSR border based on the R^2 value to aide visualization (below 0.2 not shown, R1 has the thinnest border (0.2-0.5), R2 (0.5-0.7), R3 (0.7-0.9) and R4 the thickest (≥ 0.9)). The top line in each of the relationship boxes describe the variable as a function of the other variables in the relationship. n is the number of observations, r2 is the R^2 value, ar2 is the adjusted R^2 and p is the P-values.

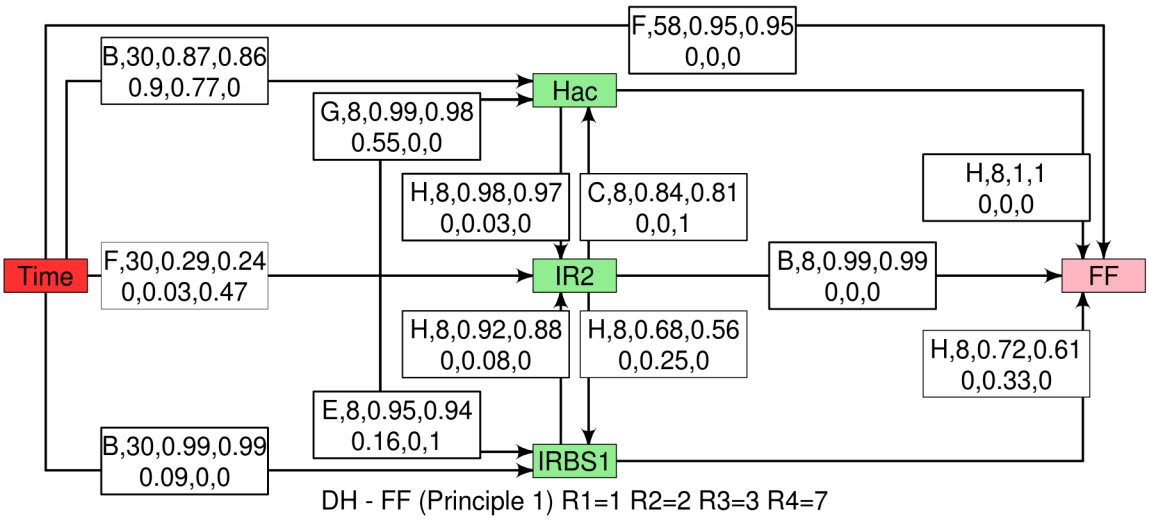

FIGURE 11. Model generated with the most relationships shown for Principle 1 for the damp heat exposure for the system response of *FF* using the unit variables of *Hac*, *IR*2 and *IRBS*1 shows 13 relationships. Information on each relationship is described in the box. The information contained is functional form, number of observations, R^2, adjusted R^2, P-value 1, P-value 2 and P-value 3, respectively. The strength of the SSR is summarized by the line width of the SSR border based on the R^2 value to aide visualization (below 0.2 not shown, R1 has the thinnest border (0.2-0.5), R2 (0.5-0.7), R3 (0.7-0.9) and R4 the thickest (≥ 0.9)). The functional forms are designated as A (simple linear), B (quadratic), C (simple quadratic), D (exponential), E (logarithmic), F (linear change point), G (nonlinearizable exponential-up) and H (nonlinearizable exponential-down).

9) INSIGHTS INTO MODULE DEGRADATION

The damp heat exposure results show very strong R^2 values for many of the "best" fitting models using Principle 1, which indicates that the observed relationships are in potential agreement with theoretical underlying physical and chemical mechanisms (Figure 7). When these relationships are evaluated with domain knowledge, they appear sensible. It is especially interesting to note the indicated strong sequential

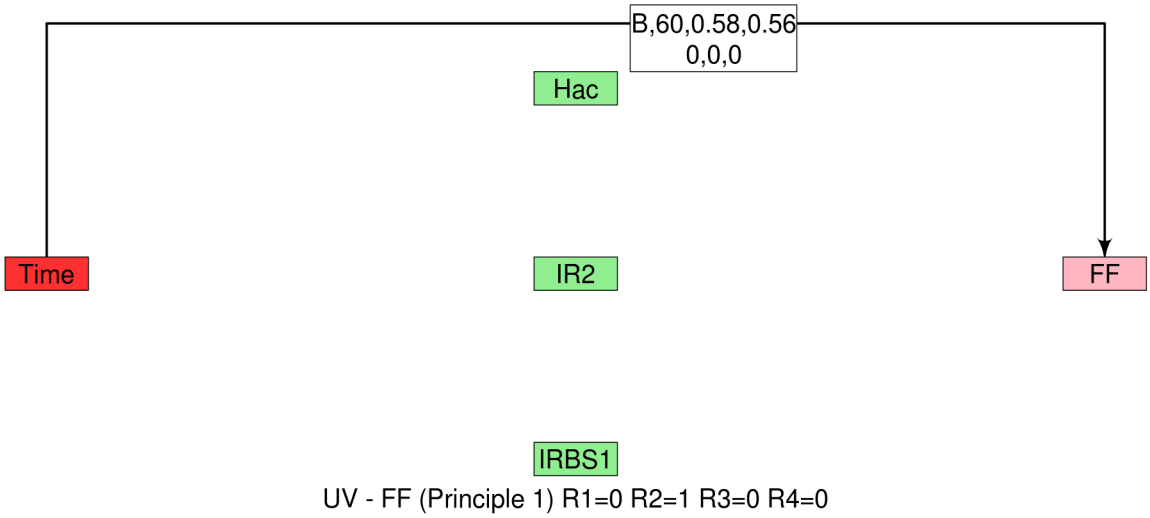

FIGURE 12. Model generated with the most relationships shown for Principle 1 for the UV exposure for the system response of *FF* using the unit variables of *Hac*, *IR*2 and *IRBS*1 shows only a relationship between *Time* and *FF*. Information on each relationship is described in the box. The information contained is functional form, number of observations, R^2, adjusted R^2, P-value 1, P-value 2 and P-value 3, respectively. The strength of the SSR is summarized by the line width of the SSR border based on the R^2 value to aide visualization (below 0.2 not shown, R1 has the thinnest border (0.2-0.5), R2 (0.5-0.7), R3 (0.7-0.9) and R4 the thickest (≥ 0.9)). The functional forms are designated as A (simple linear), B (quadratic), C (simple quadratic), D (exponential), E (logarithmic), F (linear change point), G (nonlinearizable exponential-up) and H (nonlinearizable exponential-down).

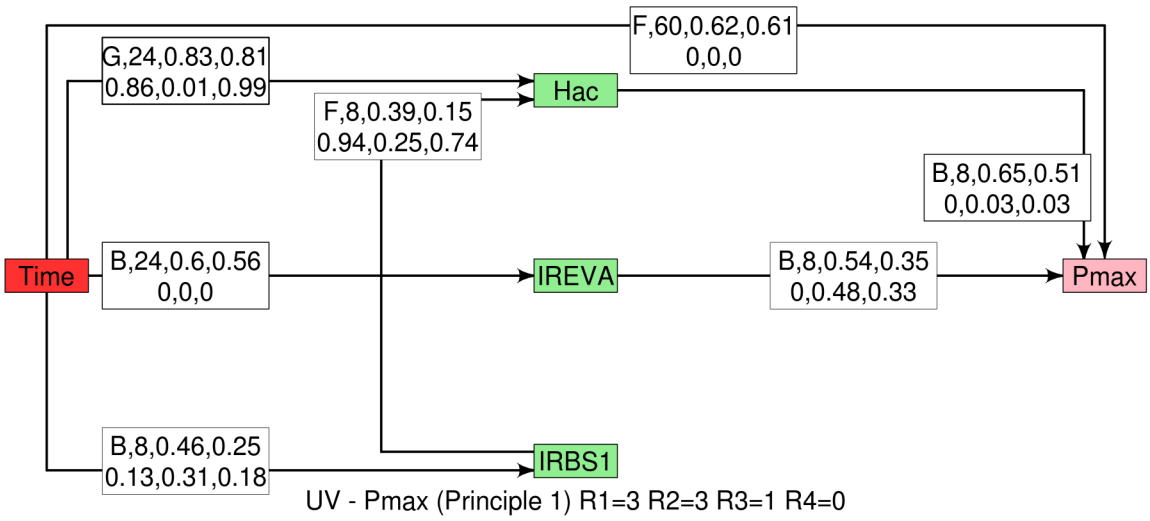

FIGURE 13. Model generated with the most relationships shown for Principle 1 for the UV exposure for the system response of *Pmax* using the unit variables of *Hac*, *IREVA* and *IRBS*1 shows 7 relationships. Information on each relationship is described in the box. The information contained is functional form, number of observations, R^2, adjusted R^2, P-value 1, P-value 2 and P-value 3, respectively. The strength of the SSR is summarized by the line width of the SSR border based on the R^2 value to aide visualization (below 0.2 not shown, R1 has the thinnest border (0.2-0.5), R2 (0.5-0.7), R3 (0.7-0.9) and R4 the thickest (≥ 0.9)). The functional forms are designated as A (simple linear), B (quadratic), C (simple quadratic), D (exponential), E (logarithmic), F (linear change point), G (nonlinearizable exponential-up) and H (nonlinearizable exponential-down).

relationship from *Time* to *IRBS*1 to *Hac* to *Pmax*. This corresponds well to the degradation pathway of PET hydrolysis leading to increased moisture ingress, which can cause an increase in EVA hydrolysis and acetic acid formation, ultimately leading to cell interconnect corrosion and power loss in the module with a change point at 1890 hours.

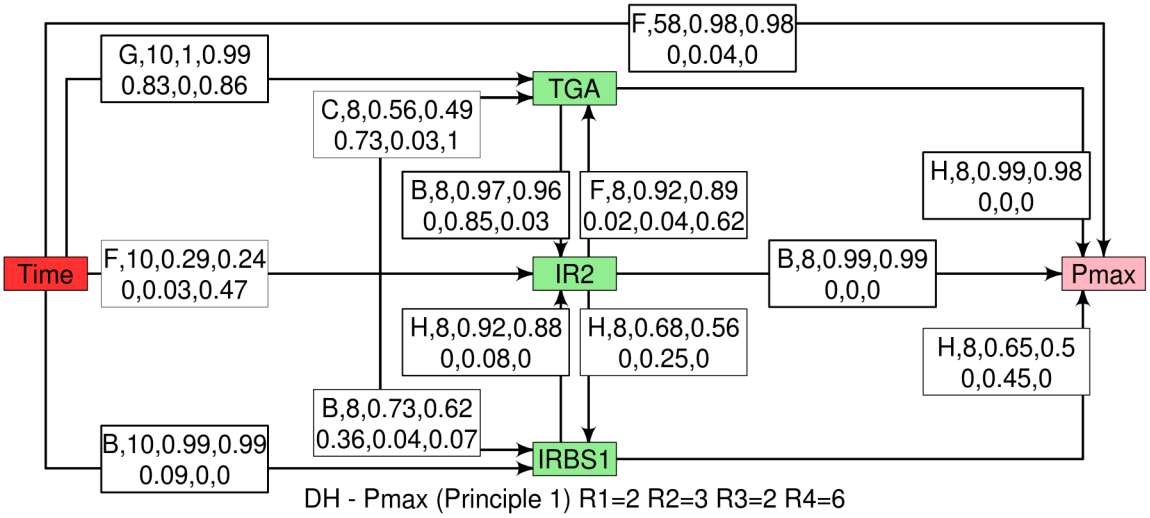

FIGURE 14. Model generated with Principle 1 for the damp heat exposure for the system response of *Pmax* using the unit variables of *TGA*, *IR*2 and *IRBS*1 shows 13 relationships. Information on each relationship is described in the box. The information contained is functional form, number of observations, R^2, adjusted R^2, P-value 1, P-value 2 and P-value 3, respectively. The strength of the SSR is summarized by the line width of the SSR border based on the R^2 value to aide visualization (below 0.2 not shown, R1 has the thinnest border (0.2-0.5), R2 (0.5-0.7), R3 (0.7-0.9) and R4 the thickest (≥ 0.9)). The functional forms are designated as A (simple linear), B (quadratic), C (simple quadratic), D (exponential), E (logarithmic), F (linear change point), G (nonlinearizable exponential-up) and H (nonlinearizable exponential-down).

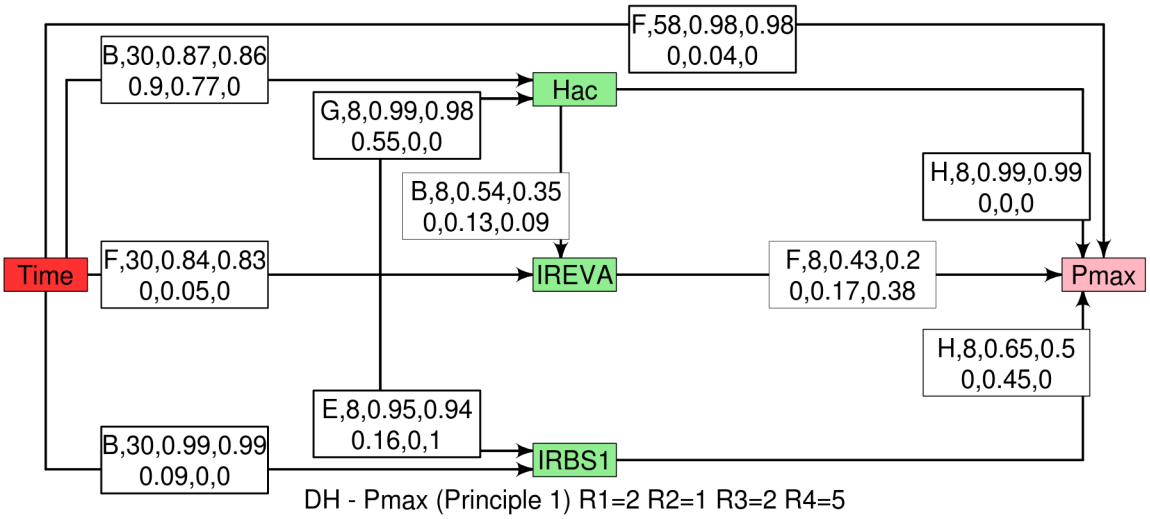

FIGURE 15. Model generated with Principle 1 for the damp heat exposure for the system response of *Pmax* using the unit variables of *Hac*, *IREVA* and *IRBS*1 shows 10 relationships. Information on each relationship is described in the box. The information contained is functional form, number of observations, R^2, adjusted R^2, P-value 1, P-value 2 and P-value 3, respectively. The strength of the SSR is summarized by the line width of the SSR border based on the R^2 value to aide visualization (below 0.2 not shown, R1 has the thinnest border (0.2-0.5), R2 (0.5-0.7), R3 (0.7-0.9) and R4 the thickest (≥ 0.9)). The functional forms are designated as A (simple linear), B (quadratic), C (simple quadratic), D (exponential), E (logarithmic), F (linear change point), G (nonlinearizable exponential-up) and H (nonlinearizable exponential-down).

The UV preconditioning exposure condition results show mediocre R^2 values for many of the "best fitting" models, which indicates that the observed relationships are in either poor agreement with theoretical underlying physics and chemistry mechanisms or the responses are flat, and not many degradation changes have occurred. Examining the nature of the response of *Pmax* through *Time* for these exposure conditions indicates that the latter is true, and the UV stress

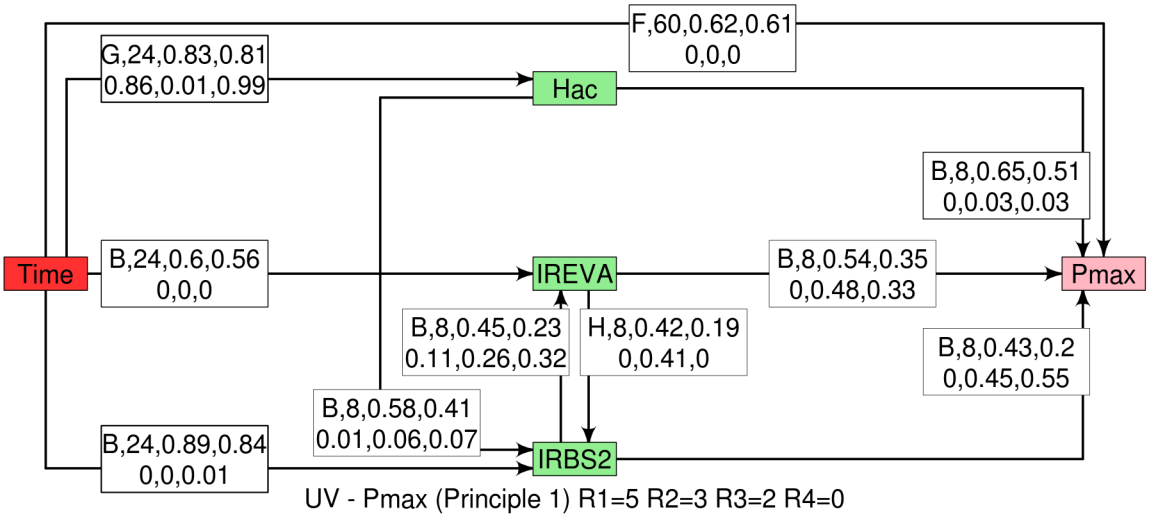

FIGURE 16. Model generated with Principle 1 for the UV exposure for the system response of *Pmax* using the unit variables of *Hac*, *IREVA* and *IRBS*2 shows 10 relationships. Information on each relationship is described in the box. The information contained is functional form, number of observations, R^2, adjusted R^2, P-value 1, P-value 2 and P-value 3, respectively. The strength of the SSR is summarized by the line width of the SSR border based on the R^2 value to aide visualization (below 0.2 not shown, R1 has the thinnest border (0.2-0.5), R2 (0.5-0.7), R3 (0.7-0.9) and R4 the thickest (≥ 0.9)). The functional forms are designated as A (simple linear), B (quadratic), C (simple quadratic), D (exponential), E (logarithmic), F (linear change point), G (nonlinearizable exponential-up) and H (nonlinearizable exponential-down).

levels were not high enough to create a measurable change in responses (Figure 9(b)). The relationships still seem sensible when evaluated with domain knowledge, and it is interesting to note the decreased role of backsheet hydrolysis in the model as indicated by a lack of SSRs connecting *IRBS*1 to the other variables (Figure 8).

VI. CONCLUSION

Although this particular data set is not big enough to make a complete prediction for 25-year lifetime guarantee of modules, it does provide the initial framework to develop a statistically valid methodology for structuring real-world and accelerated study protocols for efficient and relevant data collection. Experiments should be structured in order to provide the maximum amount of data for good statistics as well as efficient sampling. A large enough data set is required in order to gain a good statistical insight. It is beneficial to have more than one test that investigates the same degradation mode as in the case of acetic acid production. Having information on precursors, reactants and products, allows for a firmer understanding of that degradation mode within the system's performance metrics. Accelerated exposure protocols should be constructed such that there is sufficient degradation occurring so that measurements can feasibly measure significant degradation, but the accelerated exposure should also parallel real-world conditions in terms of the mechanisms at play. The activation of degradation modes by extremely harsh conditions needs to be noted so that true degradation modes can be characterized. The comprehensive PVM L&DS model needs to encompass all degradation pathways even those not activated under a particular experimental stress condition being studied. In order to understand the degradation modes, mechanisms and rates to accurately predict lifetime of PV modules, all degradation pathways need to be examined and information about these pathways elucidated and cross-correlated.

The SSR pathway for *Pmax* under the damp heat exposure corresponds well to the degradation pathway of PET hydrolysis leading to increased moisture ingress, which can cause an increase in EVA hydrolysis and acetic acid formation, ultimately leading to cell interconnect corrosion and power loss in the module with a change point at 1890 hours. UV preconditioning exposure condition results show mediocre R^2 values for many of the "best fitting' models'', which indicates that the observed relationships are in either poor agreement with theoretical underlying physics and chemistry mechanisms or the responses are flat, and not many degradation changes.

During the development of the discussed SSR networks, it was shown within the scope of the observations in this data set that certain evaluations contain more information content than other evaluations that appear to measure the same degradation mechanism. The damp heat exposure caused a large drop in the system responses compared to the less aggressive UV exposure, which did not cause much degradation to the modules. The system response *Pmax* appears to provide more information than *FF*. The development of the PVM L&DS model allows for the refinement of the model with more data

over time; therefore, with each iteration of model development, the *semi-gSEM* procedure will provide more accurate statistical results.

Traditional lifetime reliability methods do not provide a statistical means in order to accurately predict lifetime of PV modules. A procedure to determine lifetime through statistics shows statistically relevant degradation methods for different types of stressors. The procedure defined in this paper can be modified, but the idea of investigating relationships between degradation pathways and stressors without bias is important with the use of domain knowledge to guide model determination. Further model development will include nonlinear SEM or generalized SEM, so that a structure of equations can be elucidated that will guide the prediction of lifetime for PV modules in a variety of real-world conditions. The further iterations of the PVM L&DS model will contribute to reproducible open data science in PV reproducible open data science.

ACKNOWLEDGMENT

The authors acknowledge funding from Underwriter Laboratories. Research was performed at the SDLE Center at Case Western Reserve University, funded through the Ohio Third Frontier, Wright Project Program Award Tech 12-004.

SUPPLEMENTAL MATERIAL

Additional information included with this paper is a tidy data set, commented R code for the data analysis and SSR development for the tidied data set. Additionally there is a small presentation describing the *semi-gSEM* method.

REFERENCES

[1] J. Hemminger. (2012, Sep.). *From Quanta to the Continuum: Opportunities for Mesoscale Science*, The Basic Energy Sciences Advisory Committee, Besançon, France [Online]. Available: http://science.energy.gov/_/media/bes/pdf/reports/files/OFMS rpt.pdf

[2] M. P. Murray, D. Gordon, S. A. Brown, W.-C. Lin, K. A. Shell, M. A. Schuetz, S. Fowler, J. Elman, and R. H. French, "Solar radiation durability framework applied to acrylic solar mirrors," in *Proc. Rel. Photovolt. Cells, Modules, Compon., Syst. IV*, Sep. 2011, pp. 811203-1–811203-10.

[3] R. French, M. Murray, W.-C. Lin, K. Shell, S. Brown, M. Schuetz, and R. Davis, "Solar radiation durability of materials components and systems for low concentration photovoltaic systems," in *Proc. IEEE Energytech*, May 2011, pp. 1–5.

[4] R. French, J. Rodríguez-Parada, M. Yang, M. Lemon, E. Romano, and P. Boydell, "Materials for concentrator photovoltaic systems: Optical properties and solar radiation durability," in *Proc. AIP Conf.*, Apr. 2010, pp. 127–130.

[5] *International PV Module Quality Assurance Task Force, Established by NREL, AIST, PVTEC, U. S. DOE, EU JRC, SEMI PV Group to Develop PV Lifetime Qualification Testing*, NREL, Golden, CO, USA, 2012.

[6] J. Hemminger, G. Crabtree, and A. Malozemoff. (2010, Apr.). *Science for Energy Technology: Strengthening the Link Between Basic Research and Industry*. The Basic Energy Sciences Advisory Committee, US Department of Energy Besançon, France [Online]. Available: http://science.energy.gov/_/media/bes/pdf/reports/files/

[7] J. A. McLinn, "Constant failure rate—A paradigm in transition?" *Qual. Rel. Eng. Int.*, vol. 6, no. 4, pp. 237–241, Sep.–Oct. 1990.

[8] K. L. Wong, "What is wrong with the existing reliability prediction methods?" *Qual. Rel. Eng. Int.*, vol. 6, no. 4, pp. 251–257, Sep.–Oct. 1990.

[9] M. G. Pecht, "Prognostics and health management of electronics" in *Introduction*. New York, NY, USA: Wiley, 2008, pp. 1–24.

[10] M. G. Pecht, "Prognostics and health management of electronics," in *Physics-of-Failure Approach to PHM*. New York, NY, USA: Wiley, 2008, pp. 73–84.

[11] H. S. Blanks, "Arrhenius and the temperature dependence of non-constant failure rate," *Qual. Rel. Eng. Int.*, vol. 6, no. 4, pp. 259–265, 1990.

[12] M. Cushing, D. Mortin, T. Stadterman, and A. Malhotra, "Comparison of electronics-reliability assessment approaches," *IEEE Trans. Rel.*, vol. 42, no. 4, pp. 542–546, Dec. 1993.

[13] J. Gu and M. Pecht, "Prognostics and health management using physics-of-failure," in *Proc. Ann. Rel. Maintainability Symp.*, Jan. 2008, pp. 481–487.

[14] S. Cheng and M. Pecht, "A fusion prognostics method for remaining useful life prediction of electronic products," in *Proc. IEEE Int. Conf. Autom. Sci. Eng.*, Aug. 2009, pp. 102–107.

[15] B. Sun, S. Zeng, R. Kang, and M. Pecht, "Benefits analysis of prognostics in systems," in *Proc. Prognostics Health Manag. Conf.*, Jan. 2010, pp. 1–8.

[16] B. Sun, S. Zeng, R. Kang, and M. Pecht, "Benefits and challenges of system prognostics," *IEEE Trans. Rel.*, vol. 61, no. 2, pp. 323–335, Jun. 2012.

[17] D. Riley and J. Johnson, "Photovoltaic prognostics and heath management using learning algorithms," in *Proc. 38th IEEE Photovolt. Specialists Conf.*, Jun. 2012, pp. 001535–001539.

[18] Z. S. Chen, Y. Yang, and Z. Hu, "A technical framework and roadmap of embedded diagnostics and prognostics for complex mechanical systems in prognostics and health management systems," *IEEE Trans. Rel.*, vol. 61, no. 2, pp. 314–322, Jun. 2012.

[19] H.-Q. Gu, S. Zhang, and L. Ma, "Process analysis for performance evaluation of prognostics methods orienting to engineering application," in *Proc. Int. Conf. Qual., Rel., Risk, Maintenance, Safety Eng.*, Jun. 2012, pp. 681–686.

[20] N. Vichare and M. Pecht, "Prognostics and health management of electronics," *IEEE Trans. Compon. Packag. Technol.*, vol. 29, no. 1, pp. 222–229, Mar. 2006.

[21] M. Pecht and J. Gu, "Physics-of-failure-based prognostics for electronic products," *Trans. Inst. Meas. Control*, vol. 31, nos. 3–4, pp. 309–322, Jun.–Aug. 2009.

[22] M. P. Murray, L. S. Bruckman, and R. H. French, "Photodegradation in a stress and response framework: Poly(methyl methacrylate) for solar mirrors and lens," *J. Photon. Energy*, vol. 2, no. 1, p. 022004, 2012.

[23] M. Murray, L. Bruckman, and R. French, "Durability of acrylic: Stress and response characterization of materials for photovoltaics," in *Proc. IEEE Energytech*, May 2012, pp. 1–6.

[24] L. Bruckman, M. Murray, S. Richardson, S. Brown, M. Schuetz, and R. French, "Degradation of back surface acrylic mirrors: Implications for low concentration and mirror augmented photovoltaics," in *Proc. IEEE Energytech*, May 2012, pp. 1–4.

[25] D. King, W. Boyson, and J. Kratochvill, "Photovoltaic array performance model. Sandia National Laboratories, Albuquerque, New Mexico, 87185-0752," Sandia Nat. Lab., Albuquerque, NM, USA, Tech. Rep. SAND2004-3535, Dec. 2004.

[26] D. L. King, M. A. Quintana, J. A. Kratochvil, D. E. Ellibee, and B. R. Hansen, "Photovoltaic module performance and durability following long-term field exposure," *Progr. Photovolt., Res. Appl.*, vol. 8, no. 2, pp. 241–256, 2000.

[27] D. Riley and J. Johnson, "Photovoltaic prognostics and heath management using learning algorithms," in *Proc. 38th IEEE Photovolt. Specialists Conf.*, Jun. 2012, pp. 001535–001539.

[28] E. Wang, H. E. Yang, J. Yen, S. Chi, and C. Wang, "Failure modes of evaluation of PV module via materials degradation approach," in *Proc. PV Asia Pacific Expor Conf.*, 2012, pp. 1–4.

[29] DelSolar Co., *Headquarters 6 Kebei 2nd Road, Shunan Science Park, Zhunan Township*, Standard 35053, 2012.

[30] *IEC Standard 61215 Second Edition-Crystalline Silicon Terrestrial Photovoltaic (PV) Modules-Design Qualification and Type Approval*, IEC Standard 61215, 2005.

[31] B. Ketola and A. Norris, "Degradation mechanism investigation of extended damp heat aged PV module," in *Proc. 26th Eur. Photovolt. Solar Energy Conf. Exhibit.*, 2011, pp. 3523–3528.

[32] K. Whitfield, A. Salomon, S. Yang, and I. Suez, "Damp heat versus field reliability for crystalline silicon," in *Proc. 38th IEEE Photovolt. Specialists Conf.*, Jun. 2012, pp. 001864–001870.

[33] S. Sakamoto, T. Kobayashi, and S. Nonomura, "Epidemiological analysis of degradation in silicon photovoltaic modules," *Jpn. J. Appl. Phys.*, vol. 51, no. 10, pp. 10NF03-1–10NF03-4, 2012.

[34] F. Pern, "Factors that affect the EVA encapsulant discoloration rate upon accelerated exposure," *Solar Energy Mater. Solar Cells*, vols. 41–42, pp. 587–615, Jun. 1996.
[35] G. Jorgensen, K. Terwilliger, S. Glick, J. Pern, and T. McMahon, "Materials testing for PV module encapsulation," in *Proc. Nat. Center Photovolt. Solar Program Rev. Meeting*, Mar. 2003, pp. 24–26.
[36] F. Pern and S. Glick, "Adhesion strength study of EVA encapsulants on glass substrates," in *Proc. NCPV Solar Program Rev. Meeting*, May 2003, pp. 1–4.
[37] A. Czanderna and F. Pern, "Encapsulation of PV modules using ethylene vinyl acetate copolymer as a pottant: A critical review," *Solar Energy Mater. Solar Cells*, vol. 43, no. 2, pp. 101–181, 1996.
[38] G. Oreski and G. Wallner, "Delamination behaviour of multilayer films for PV encapsulation," *Solar Energy Mater. Solar Cells*, vol. 89, no. 2, pp. 139–151, 2005.
[39] W. Stark and M. Jaunich, "Investigation of ethylene/vinyl acetate copolymer (EVA) by thermal analysis DSC and DMA," *Polymer Test.*, vol. 30, no. 2, pp. 236–242, 2011.
[40] M. Sadok and A. Mehdaoui, "Outdoor testing of photovoltaic arrays in the Saharan region," *Renew. Energy*, vol. 33, no. 12, pp. 2516–2524, 2008.
[41] J. Foreman, S. Sauerbrunn, and C. Marcozzi, *Thermal Analysis & Rheology*. Kisarazu, Japan: Kyoritsu Chem. & Co., Ltd., Mar. 2013.
[42] M. Hidalgo, F. Medlege, M. Vite, C. Corfias-Zuccalli, P. Voarino, and J. Gonzalez-Leon, "New DSC method for the quality control of PV modules: Simple and quick determination of the cross-linking degree of EVA encapsulants, and other properties," p. 130, Nov. 2011.
[43] B. Ketola and A. Norris, "The role of encapsulant moisture permeability in the durability of solar photovoltaic modules," in *Proc. 25th Eur. Photovolt. Solar Energy Conf. Exhibit.*, 2010, pp. 1–9.
[44] T. Swonke and R. Auer, "Impact of moisture on PV module encapsulants," in *Proc. SPIE, Rel. Photovolt. Cells, Modules, Compon., Syst. II*, vol. 7412, pp. 74120A-1–74120A-7, Aug. 2009.
[45] G. Jorgensen, K. Terwilliger, G. Barber, C. Kennedy, and T. McMahon, "Measurements of backsheet moisture permeation and encapsulant-substrate adhesion," in *Proc. NCPV Program Rev. Meeting*, 2001, pp. 14–17.
[46] T. Shioda, "Amount of desorbed acetic acid in EVA during DH test and long-term outdoor exposure and its influence on module performances," in *Proc. NREL PV Module Rel. Workshop*, 2012, pp. 1–6.
[47] P. Klemchuk, M. Ezrin, G. Lavigne, W. Holley, J. Galica, and S. Agro, "Investigation of the degradation and stabilization of EVA-based encapsulant in field-aged solar energy modules," *Polymer Degradation Stability*, vol. 55, no. 3, pp. 347–365, 1997.
[48] S. Tambe, S. Singh, M. Patri, and D. Kumar, "Ethylene vinyl acetate and ethylene vinyl alcohol copolymer for thermal spray coating application," *Progr. Organic Coatings*, vol. 62, no. 4, pp. 382–386, 2008.
[49] M. C. Costache, D. D. Jiang, and C. A. Wilkie, "Thermal degradation of ethylene–vinyl acetate coplymer nanocomposites," *Polymer*, vol. 46, no. 18, pp. 6947–6958, Aug. 2005.
[50] G. Oreski and K. Möller, "Qualification of polymeric components for use in PV modules," in *Proc. SPIE, Rel. Photovolt. Cells, Modules, Compon., Syst. IV*, vol. 8112, p. 81120B, Sep. 2011.
[51] C. Sammon, J. Yarwood, and N. Everall, "An FT–IR study of the effect of hydrolytic degradation on the structure of thin PET films," *Polymer Degradation Stability*, vol. 67, no. 1, pp. 149–158, Jan. 2000.
[52] G. Oreski and G. Wallner, "Aging mechanisms of polymeric films for PV encapsulation," *Solar Energy*, vol. 79, no. 6, pp. 612–617, 2005.
[53] A. F. Zielnik and D. P. Dumbleton, "Photovoltaic module weather durability & reliability: Will my module last outdoors?" Ph.D. dissertation, Dept. Solar Energy Competence Center, Atlas Mater. Test. Technol. LLC, Chicago, IL,USA, Jun. 2012.
[54] M. Kempe, "Overview of scientific issues involved in selection of polymers for PV applications," in *Proc. 37th IEEE Photovolt. Specialists Conf.*, Jun. 2011, pp. 000085–000090.
[55] R Development Core Team, *R: A Language and Environment for Statistical Computing*, Vienna, Austria: R Found. Stat. Comput., 2008, p. 409.
[56] R. Kline, *Principles and Practice of Structural Equation Modeling*. New York, NY, USA: Guilford Press, 2010.
[57] D. Hooper, J. Coughlan, and M. Mullen, "Structural equation modelling: Guidelines for determining model fit," *Electron. J. Bus. Res. Methods*, vol. 6, no. 1, pp. 53–60, 2008.
[58] K. Preacher and E. Merkle, "The problem of model selection uncertainty in structural equation modeling." *Psychol. Methods*, vol. 17, no. 1, p. 1, 2012.
[59] J. J. Faraway, *Linear Models with R*. London, U.K.: Chapman & Hall, 2004.
[60] S. Weisberg, *Applied Linear Regression* (Wiley Series in Probability and Statistics). New York, NY, USA: Wiley, 2005.
[61] R. Bagozzi and Y. Yi, "Specification, evaluation, and interpretation of structural equation models," *J. Acad. Marketing Sci.*, vol. 40, no. 1, pp. 8–34, 2012.
[62] F. Pern, "Factors that affect the EVA encapsulant discoloration rate upon accelerated exposure," in *Proc. IEEE 1st World Conf. Photovolt. Energy Convers., Conf. Rec. 24th IEEE Photovolt. Specialists Conf.*, vol. 1. Dec. 1994, pp. 897–900.
[63] F. Pern and S. Glick, "Photothermal stability of encapsulated Si solar cells and encapsulation materials upon accelerated exposures," *Solar Energy Mater. Solar Cells*, vol. 61, no. 2, pp. 153–188, 2000.
[64] W. Gambogi, "Comparative performance of backsheets for photovoltaic modules," in *Proc. 25th Eur. Photovolt. Solar Energy Conf. Exhibit.*, Sep. 2010, pp. 4079–4083.
[65] J. Del Cueto and T. McMahon, "Analysis of leakage currents in photovoltaic modules under high-voltage bias in the field," in *Proc. Progr. Photovolt., Res. Appl.*, vol. 10, no. 1, pp. 15–28, Jan. 2002.
[66] D. Jordan, M. Kempe, D. Miller, C. Packard, J. Wohlgemuth, and S. Kurtz, "Observed field failures and reported degradation rates," in *Proc. NREL Thin Film PV Workshop*, Feb. 2013, pp. 1–4.
[67] J. Elerath and M. Pecht, "IEEE 1413: A standard for reliability predictions," *IEEE Trans. Rel.*, vol. 61, no. 1, pp. 125–129, Mar. 2012.
[68] P. Dalgaard, *Introductory Statistics with R* (Statistics and Computing), New York, NY, USA: Springer-Verlag, 2008.
[69] S. Boslaugh and P. Watters, *Statistics in a Nutshell: A Desktop Quick Reference*. Sebastopol, CA, USA: O'Reilly Media, 2009.

LAURA S. BRUCKMAN is a Research Associate at Case Western Reserve University (CWRU), Cleveland, OH, USA. She received the Ph.D. degree in analytical chemistry from the University of South Carolina, Columbia, SC, USA, in August 2011. Her research with the University of South Carolina focused on developing methods for the rapid classification of phytoplankton cells using single-cell fluorescence measurements, optical trapping, and multivariate optical computing. Her work at CWRU has been focused on the degradation mechanisms of acrylic and acrylic back surface mirrors to apply the stress and response framework in lifetime and degradation science. Her research experiences bring together statistical analytics with big data type problems.

NICHOLAS R. WHEELER is currently pursuing the Ph.D. degree with the Solar Durability and Lifetime Extension Center, Case Western Reserve University (CWRU), Cleveland, OH, USA. He received the M.S. degree in macromolecular science and engineering from CWRU. His work with the SDLE Center involves developing prognostic models for PV module degradation under real-time and accelerated stress exposures, with special focus towards the role of polymeric subsystems such as backsheet assemblies.

JUNGHENG MA received the Ph.D. degree in statistics from Case Western Reserve University, Cleveland, OH, USA. His current research interests include clustering and classification, Bayesian inference, sampling techniques, and sample size determination.

ETHAN WANG received the M.S. degree in chemistry from National Tsing Hau University, Hsinchu, Taiwan, in 2002. He joined Underwriters Laboratories Corporate Research Team, Northbrook, IL, USA, in 2005, as a Research Scientist. His experience focused on aging and characterization of polymeric materials. Since 2007, he has been conducting research related to the reliability of PV modules and PV materials. His work involves accelerated aging on PV grounding connectors, characterization of PV encapsulation and backsheets, PV failure modes analysis, as well as outdoor weathering of PV and CPV modules.

CARL K. WANG is a Research Manager of corporate research with Underwriters Laboratories Taiwan Co., Ltd., Taipei, Taiwan, responsible for managing UL Corporate Research activities, Taiwan. His team focuses on materials science research for the safety aspects of various applications, such as battery, bio-fuel, photovoltaics, wire & cable, and PCB.

IVAN CHOU received the M.S. degree in applied chemistry from National Chiao Tung University, Hsinchu, Taiwan, in 1992. He joined Delsolar Co., Ltd., Miaoli, Taiwan, in 2010, as a Senior Manager of Quality Engineering Department. Before with PV industry, his experience was in flat panel displays with a focus on the process integration and materials analysis of TFT, LCD, and OLED. Since 2010, he has been conducting activities related to failure analysis and reliability evaluation of PV modules. His work involves PV failure modes identification, outdoor weathering of PV modules, and lifetime prediction model development.

JIAYANG SUN is a Professor of statistics and the Director of SR2C, statistical research, computing and collaboration with the Department of Epidemiology and Biostatistics, Case Western Reserve University, Cleveland, OH, USA. She received the Ph.D. degree in statistics from Stanford University, Stanford, CA, USA. She is a fellow of the American Statistical Association, the Institute of Mathematical Statistics, and a member of International Statistical Institute. His current research interests include statistical methodology, theory and computing, notably in simultaneous inference and multiple testing, biased sampling and measurement error problems, mixtures and image analysis, bioinformatics, data mining, and large, high-dimensional data analysis, statistical computing and graphical methods, semiparametrics, and random fields. Her interdisciplinary work includes research in astronomy, computer science, environment, imaging, materials science, neuroscience, and other medical sciences.

ROGER H. FRENCH is a F. Alex Nason Professor with the Department of Materials Science and Engineering. He joined Case Western Reserve University (CWRU), Cleveland, OH, USA, in August 2010, after 24 years of conducting basic research and technology development in DuPont's Central Research. He is the Director of the Solar Durability and Lifetime Extension Center, CWRU. He has a broad experience in developing and commercializing optical materials for many different applications and in optimizing these materials for improved radiation durability and lifetime. He is a nationally recognized expert in Lifetime and Degradation Science for commercial applications, evidenced by his work on attenuating phase shift photomasks, fluoropolymer pellicles for photolithography, immersion lithography imaging fluids, and materials for concentrating photovoltaic systems. He has published 22 issued patents and more than 145 publications.